

5. Results

5.1 Surface Evaluation for Protein and Antibody Microarrays

Dilution rows of anti-fibrinogen antibodies ranging from 1.26 mg/ml to 750 ng/ml and HSA ranging from 0.56 mg/ml to 0.33 μ g/ml were spotted in two identical fields, each comprising twenty replicates of every dilution row. The slides were incubated first with 4 μ g/ml labelled Cy3-fibrinogen and 3.5 μ g/ml of mouse monoclonal anti-HSA antibodies, followed by incubation with 1.3 μ g/ml Cy5-labelled goat anti-mouse IgG (Figure 10).

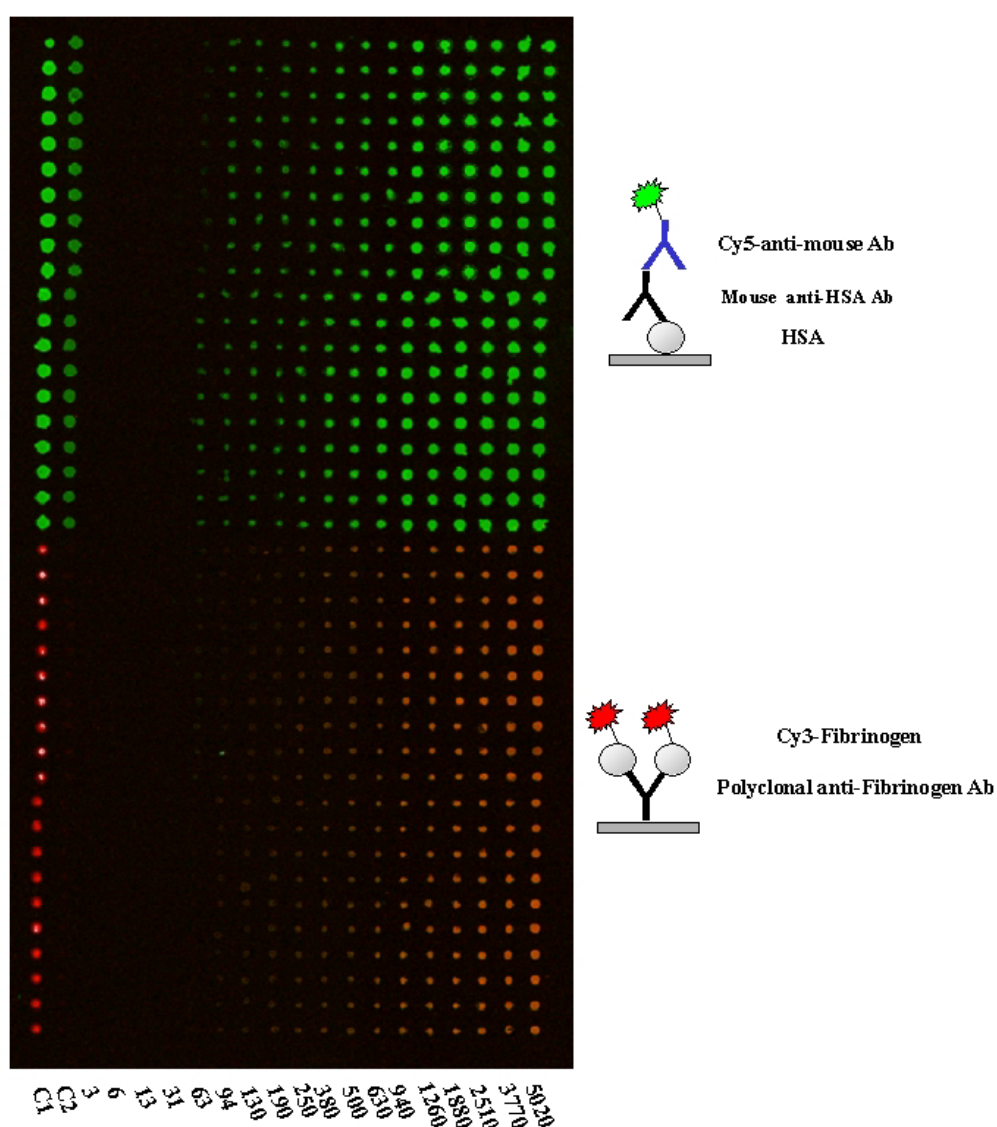


Figure 10: Spatial arrangement of the dilution rows. The schematic assembly of the molecules is demonstrated next to the scan. The numbers below the scan indicate the spotted amount of capture molecules in amol/spot

After scanning, all slides were checked for proper spotting and aberrant spots were taken out of analysis. Mean values of all replicates were calculated and a graph of mean signal intensity versus spotted concentration was generated displaying binding characteristics of each microarray support for the generation of protein (Figure 11) and antibody microarrays (Figure 12). The average coefficient of variation for each slide coating was calculated by:

$$\text{Coefficient of Variation} = \frac{\text{Standard Deviation}}{\text{Mean}}$$

excluding signal intensities below a defined cut-off in the range of background fluorescence, to prevent a deviation of the coefficient due to random effects (Table 2). The detection limit was defined as the lowest concentration at which the mean of signal intensities lay above the cut-off used in the calculation of the coefficient of variation. The mean value of the detection limits of all replicates as well as the standard deviation was calculated for protein (Figure 13) and antibody microarrays (Figure 14). No standard deviation indicates that the detection limit of all replicates was the same.

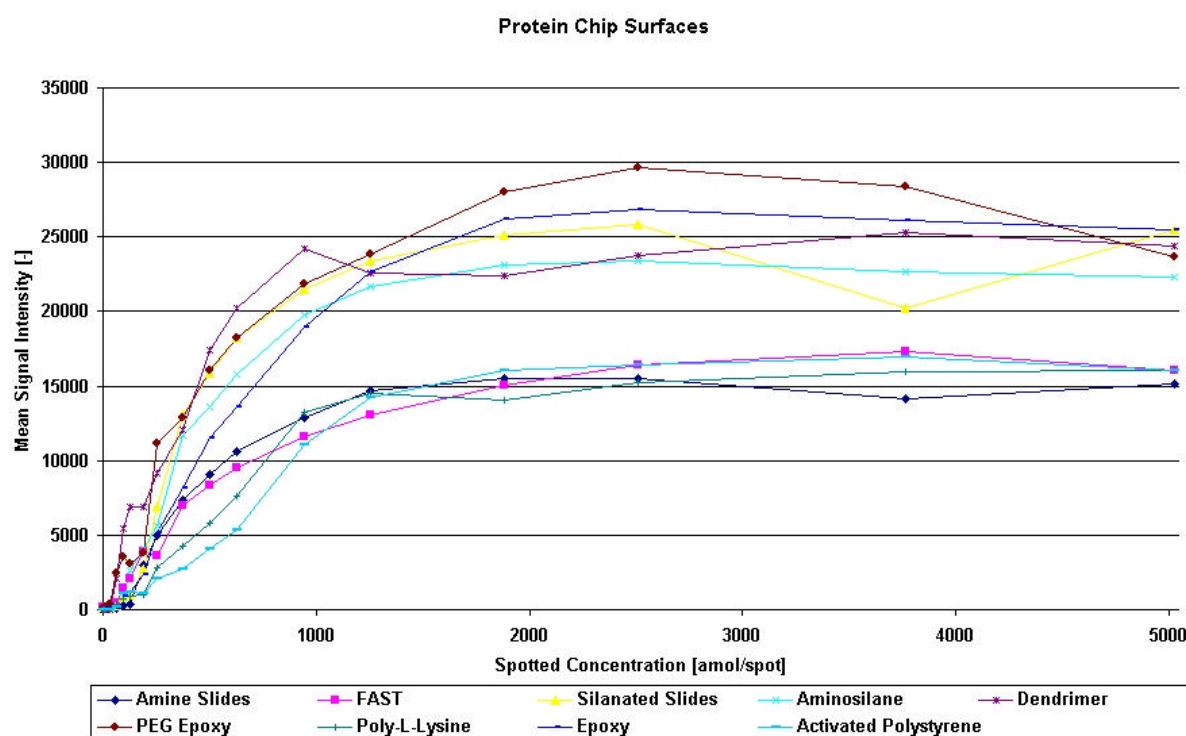


Figure 11: Graph of mean signal intensity versus spotted concentration of protein chip surfaces

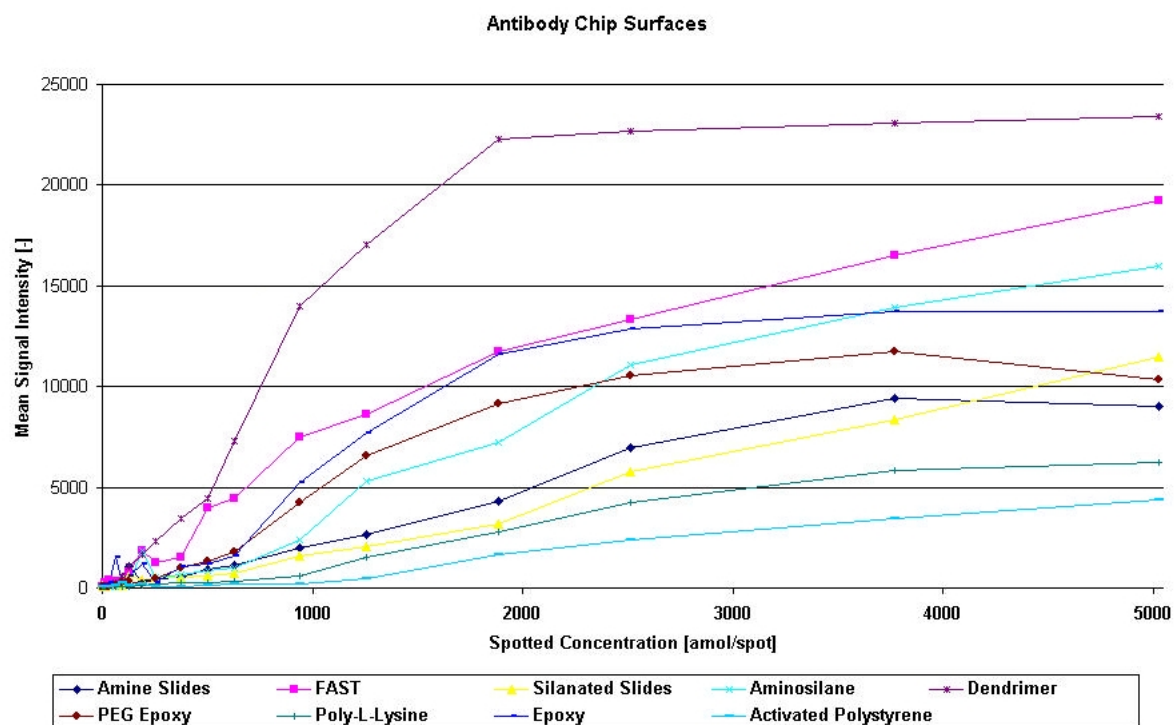


Figure 12: Graph of mean signal intensity versus spotted concentration of antibody chip surfaces

Coefficients of Variation			
	Antibody Chips	Protein Chips	Average
Dendrimer Slides	24%	21%	22%
PEG Epoxy Slides	24%	25%	24%
Poly-L-lysine Slides	35%	16%	26%
Amine Slides	41%	21%	31%
FAST Slides	32%	30%	31%
Activated Polystyrene Slides	41%	26%	33%
Epoxy Slides	43%	24%	34%
Aminosilane slides	45%	29%	37%
Silanated Slides	35%	40%	38%

Table 2: Coefficients of variation for protein and antibody microarrays

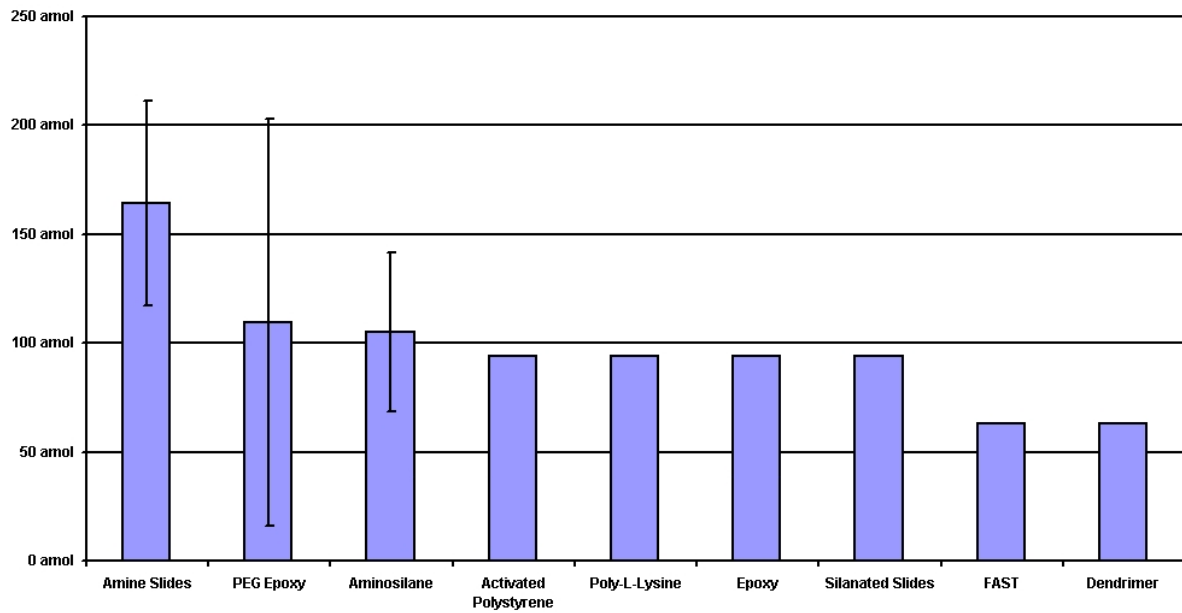


Figure 13: Detection limits of protein chip surfaces with standard deviation error bars

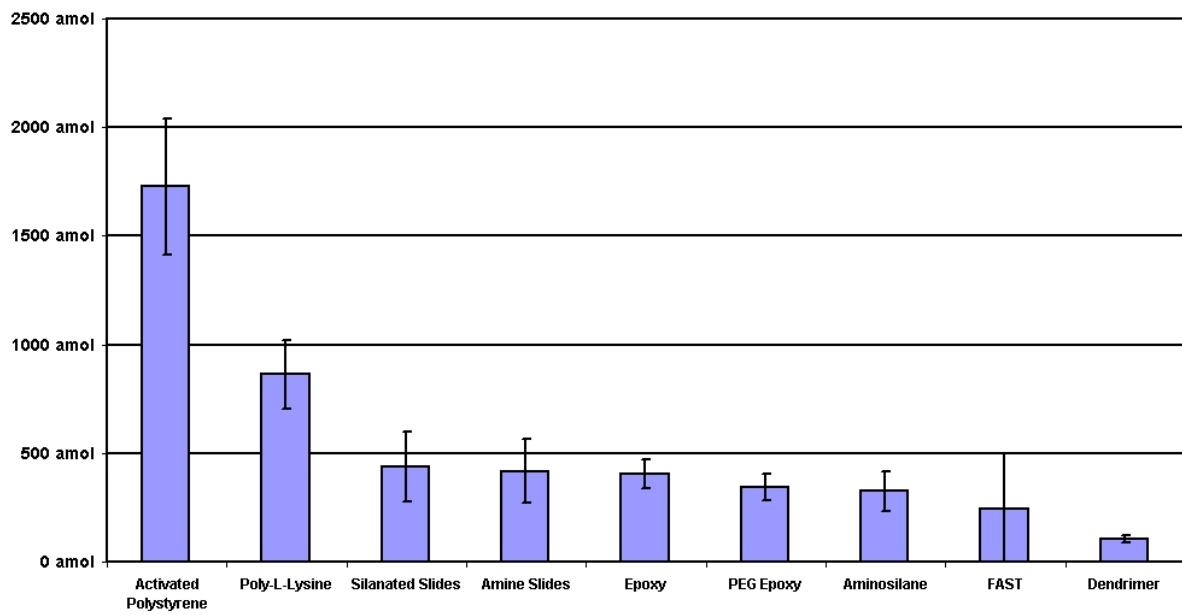


Figure 14: Detection limits of antibody chip surfaces with standard deviation error bars

5.2 Multiple Spotting Technique

The multiple spotting technique (MIST) is based on the transfer of several reaction entities to the same position on the slide. In contrast to common microarray techniques, in which only one spotting step is performed for immobilisation of substances onto a surface, MIST applies the microarray robot not only for immobilisation, but also for transfer of substances that should interact with the immobilised binder.

5.2.1 Optimisation of Production Parameters

5.2.1.1 Pin Coefficients for Immunosorbent Assay

The observation that spotting of the same batch of labelled protein resulted in different signal intensities between different pins required optimisation of the technique to produce reliable results in absolute measurements. Two different ways of optimisation were possible: the first possibility was optimisation of the hardware, which meant the manual selection of a subset of pins, to produce relatively homogeneous signal intensities. The second possibility was automatic adjustment of all results by software. Since the first approach would have been an expensive and time consuming approach, the optimisation was done using the software and pin coefficients.

To assess the quality of printing, a uniform dilution of 2 µg/ml of Cy3-labelled anti-rabbit IgG was spotted multiple times on poly-L-lysine coated slides using two different spotting heads carrying 16 either 150-micron or 100-micron solid pins (Figure 15). The arithmetic mean of all signal intensities produced by each pin was calculated and the average signal intensity of all 16 mean values was defined as 100%. For both heads, a graph indicating the relative deviations from this mean was obtained for each pin (Figure 16, Figure 17). Deviations in signal intensities of up to 41% were observed.

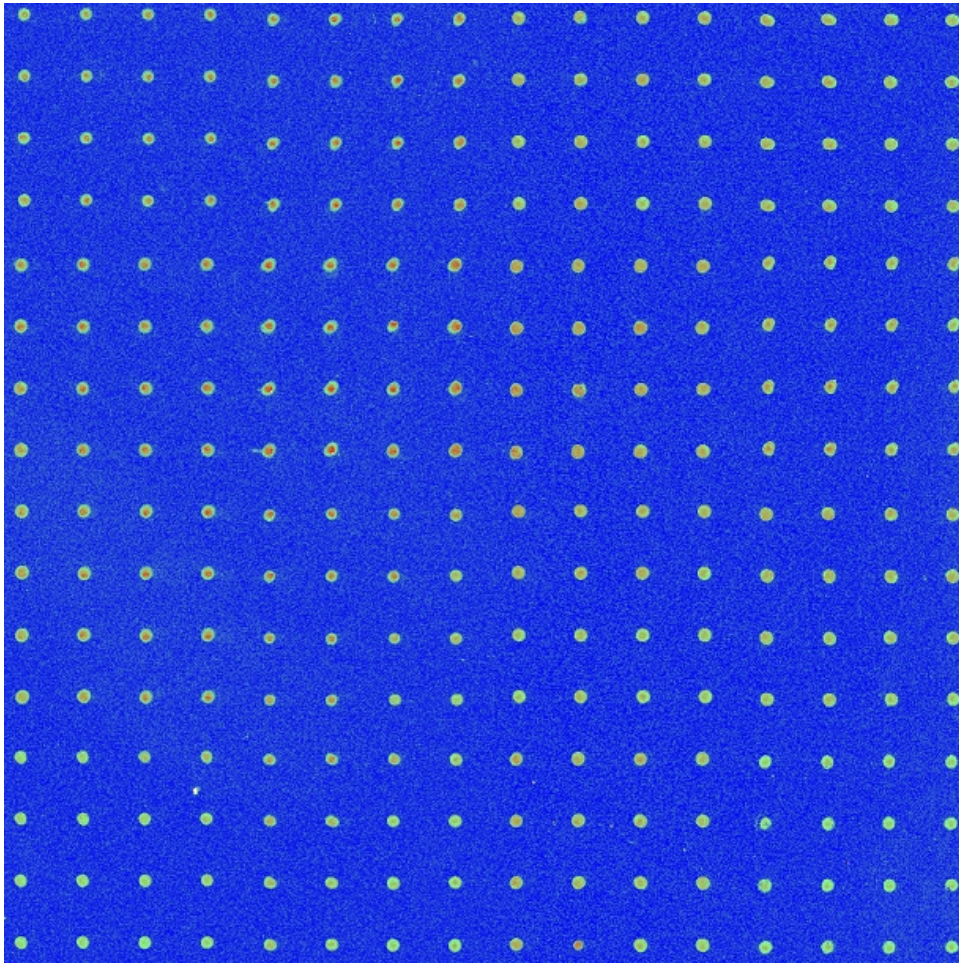


Figure 15: Scan of one microarray used for determination of pin coefficients

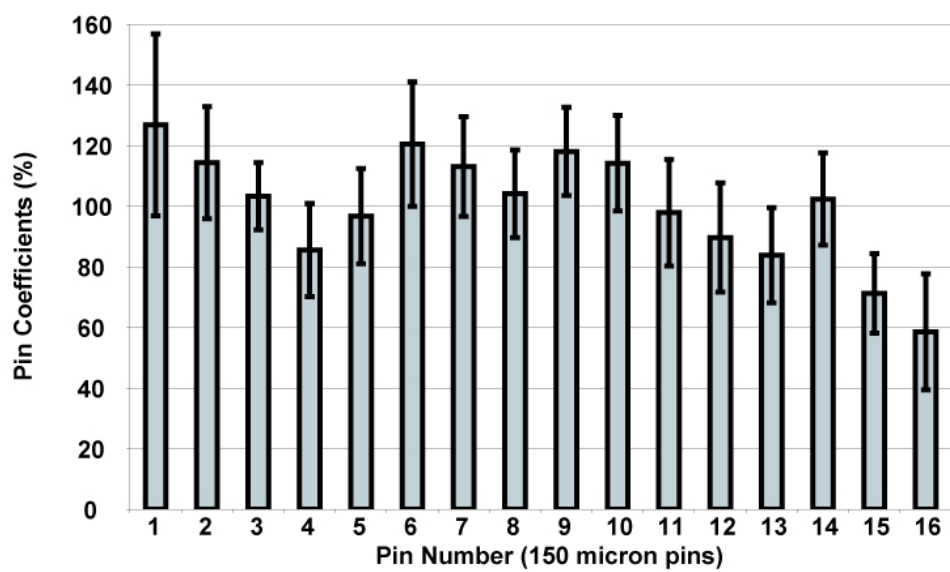


Figure 16: Pin coefficients for 150 micron pins

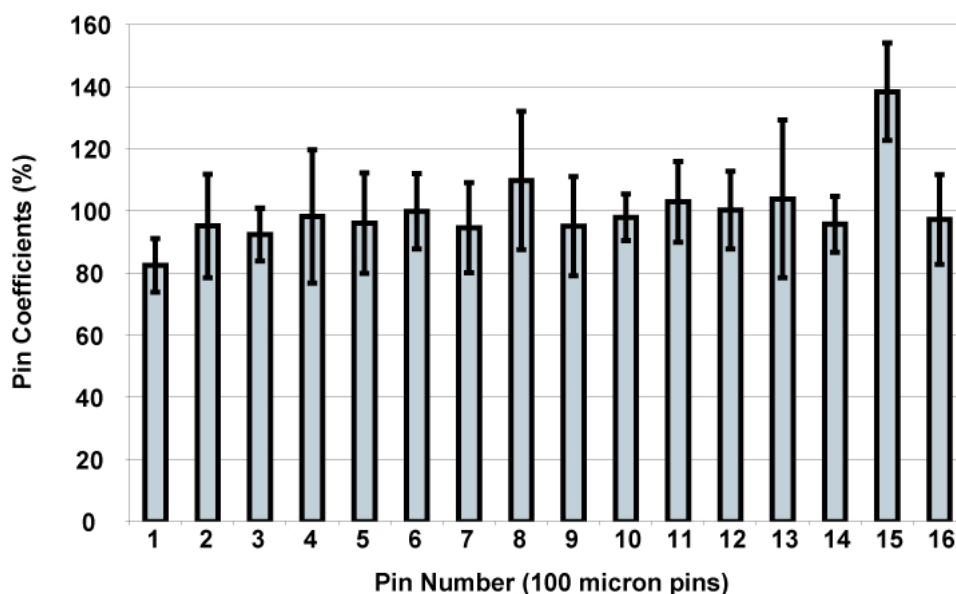


Figure 17: Pin coefficients for 100 micron pins

5.2.1.2 *Immunosorbent Assay*

One of the most important features of the multiple spotting technique is the buffer, which is used for the transfer of substances onto the immobilised binder. Apart from BSA and PBS, three hygroscopic substances (glycerol, PEG 3350 and betaine) were tested as components of the MIST-buffer. These substances should conserve a humid environment on the spot in which all reaction partners can disperse freely.

For the evaluation of betaine, 104 $\mu\text{g/ml}$ of monoclonal anti-HSA antibodies were spotted in a first spotting step onto poly-L-lysine coated slides. In a second spotting step, 20 $\mu\text{g/ml}$ of Cy5-labelled HSA containing different concentrations of betaine were spotted onto the immobilised anti-HSA antibodies (Figure 18). Negative controls of 20 $\mu\text{g/ml}$ of Cy5-labelled HSA were spotted twice in two 4x4 spot-squares at the bottom left corner; the upper one onto immobilised antibodies, the lower one onto blocked surface.

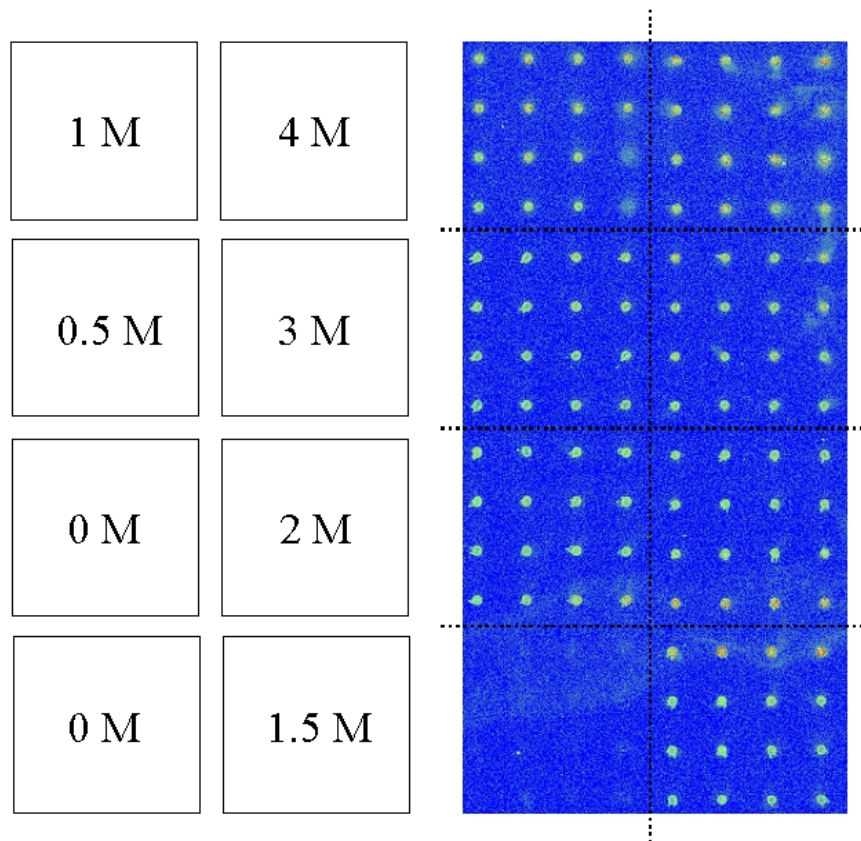


Figure 18: Scan of an antibody chip used for the screening of different betaine concentrations in the MIST-buffer

For analysis, mean values of two slides, displaying two set-ups each, were taken. A diagram of average signal intensity versus betaine concentration was drawn with standard deviation error bars (Figure 19).

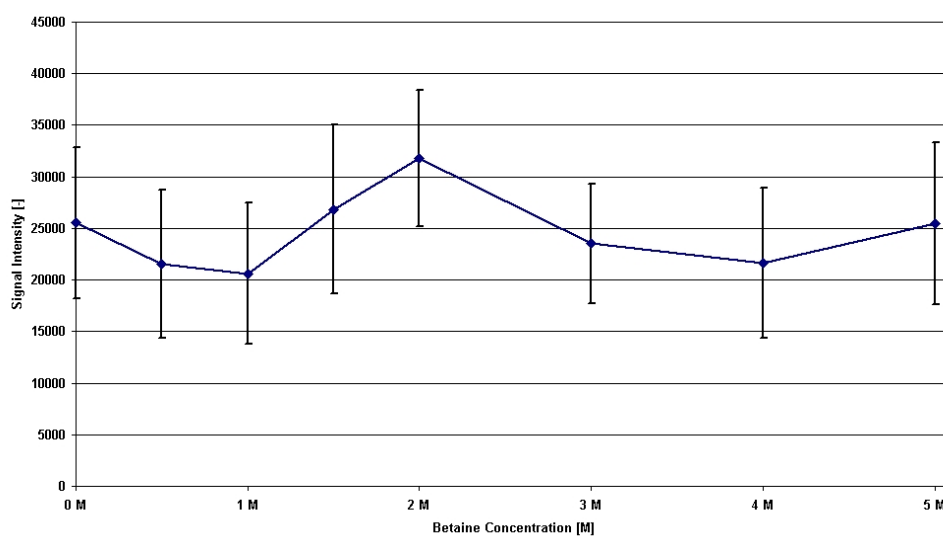


Figure 19: Diagram of average signal intensity versus betaine concentration

For the evaluation of PEG 3350 and glycerol, 104 $\mu\text{g/ml}$ of monoclonal anti-HSA antibodies were spotted onto poly-L-lysine coated slides and dilution rows of Cy5-labelled HSA ranging from 0.25 $\mu\text{g/ml}$ to 2 $\mu\text{g/ml}$ were prepared and spotted using either concentrations of 0% to 4% (w/v) PEG 3350 (Figure 20) or 0% to 8% (v/v) glycerol (Figure 22) in the spotting buffer. For analysis the mean value of each square was taken and diagrams of average signal intensity versus Cy5-labelled HSA concentrations with standard deviations for different PEG 3350 (Figure 21) or glycerol (Figure 23) concentrations were drawn.

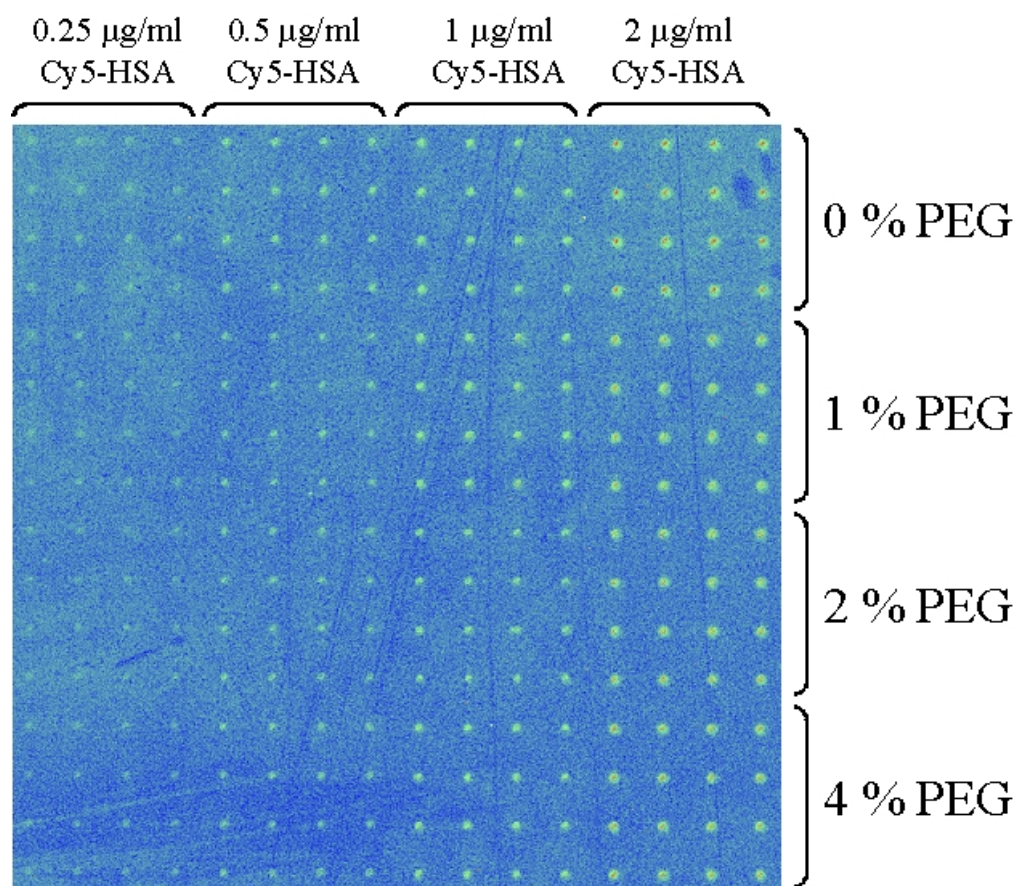


Figure 20: Scan of an antibody chip used for the screening of different PEG concentrations in the MIST-buffer

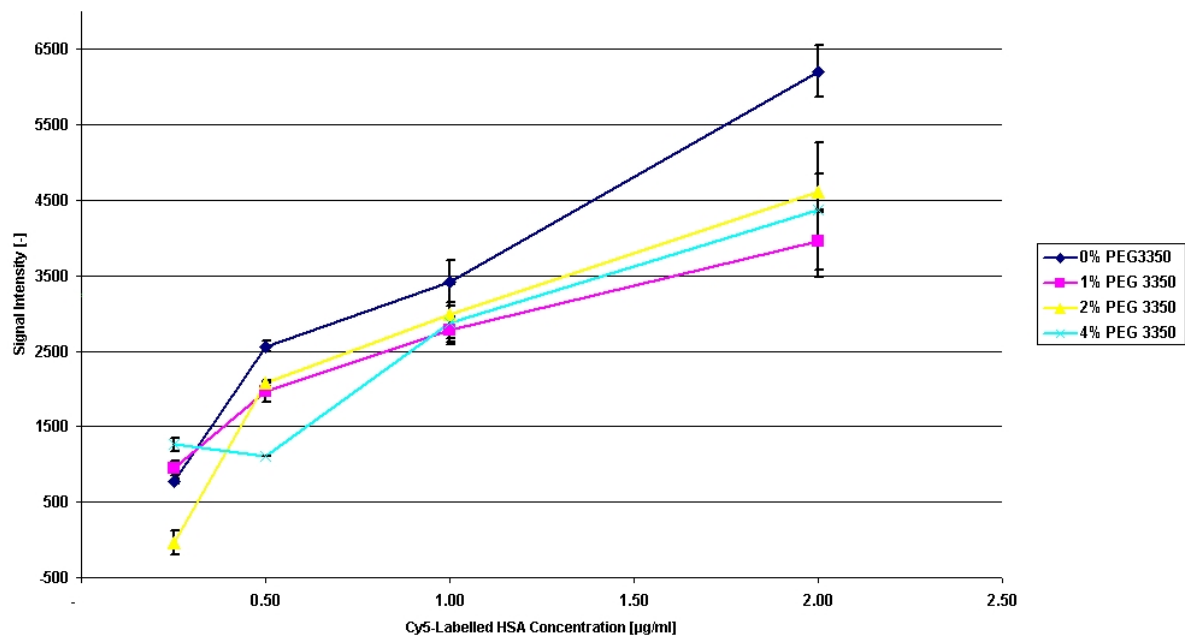


Figure 21: Diagram of average signal intensity versus Cy5-labelled HSA concentration for different PEG 3350 concentrations

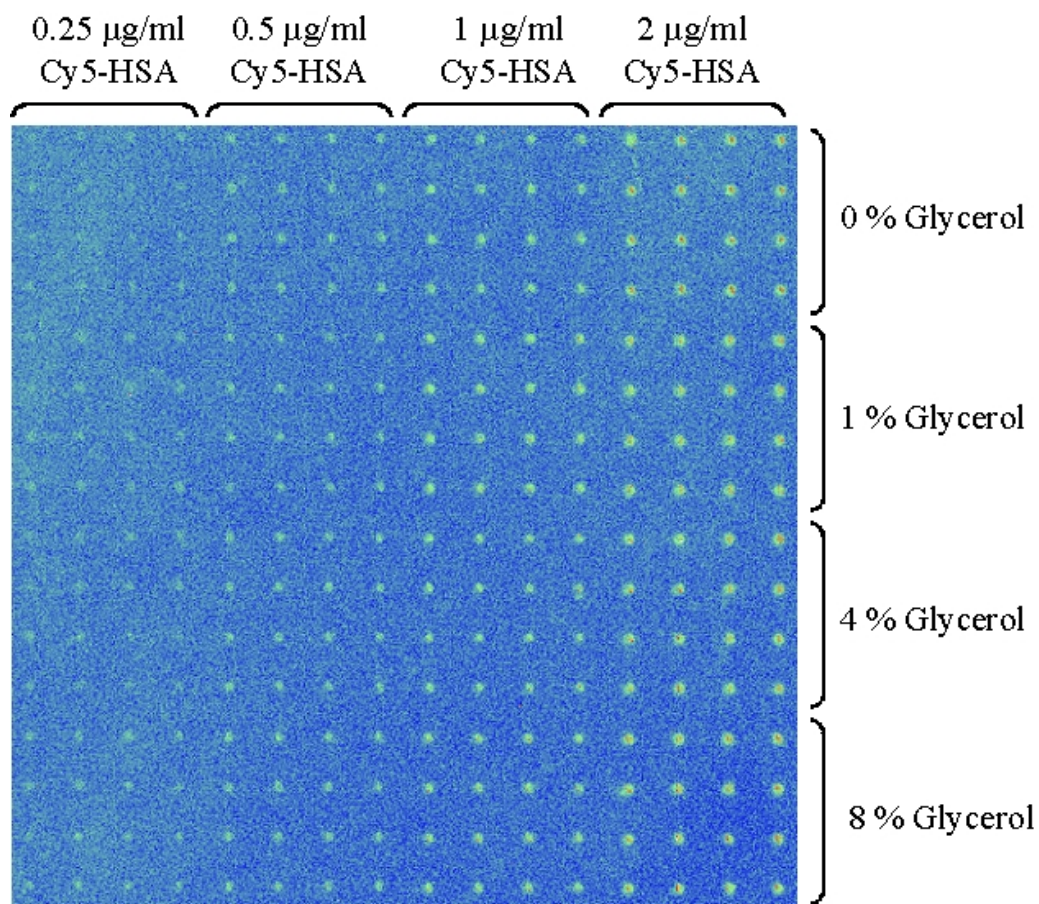


Figure 22: Scan of an antibody chip used for the screening of different glycerol concentrations in the MIST-buffer

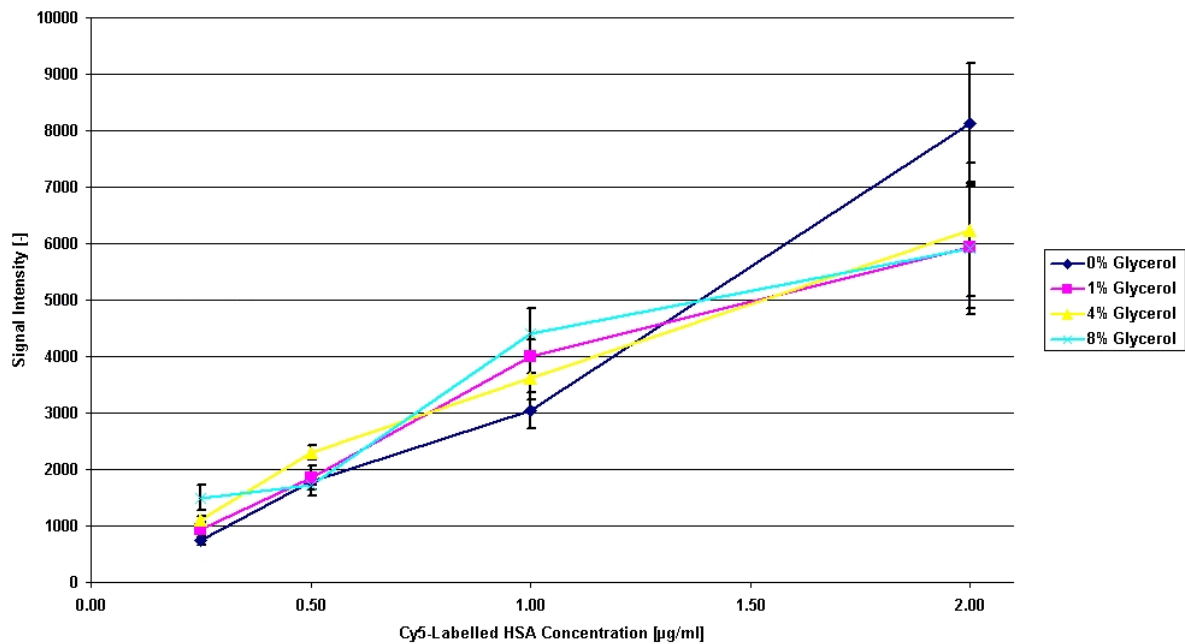


Figure 23: Diagram of average signal intensity versus Cy5-labelled HSA concentration for different glycerol concentrations

5.2.1.3 *ScFv Screening Assay*

The screening of scFv's on microarrays requires optimisation of several parameters, such as washing procedure, concentration of proteins for immobilisation and strain applied for expression.

For optimisation of the washing procedure two different washing solutions were tested. Figure 24 shows a scan of two slides, which were used for the screening of 30 monoclonal anti-poly-ubiquitin scFv's. Poly-ubiquitin with three ubiquitin moieties was spotted at a concentration of 20 $\mu\text{g/ml}$ on the top half of epoxy-coated slides, while 20 $\mu\text{g/ml}$ of HSA was spotted on the bottom half. In a second spotting step, scFv fragments were spotted on both areas of the slide. Both slides were treated identically, with the exception that slide A was washed with TBS-T and slide B with TBS-TT.

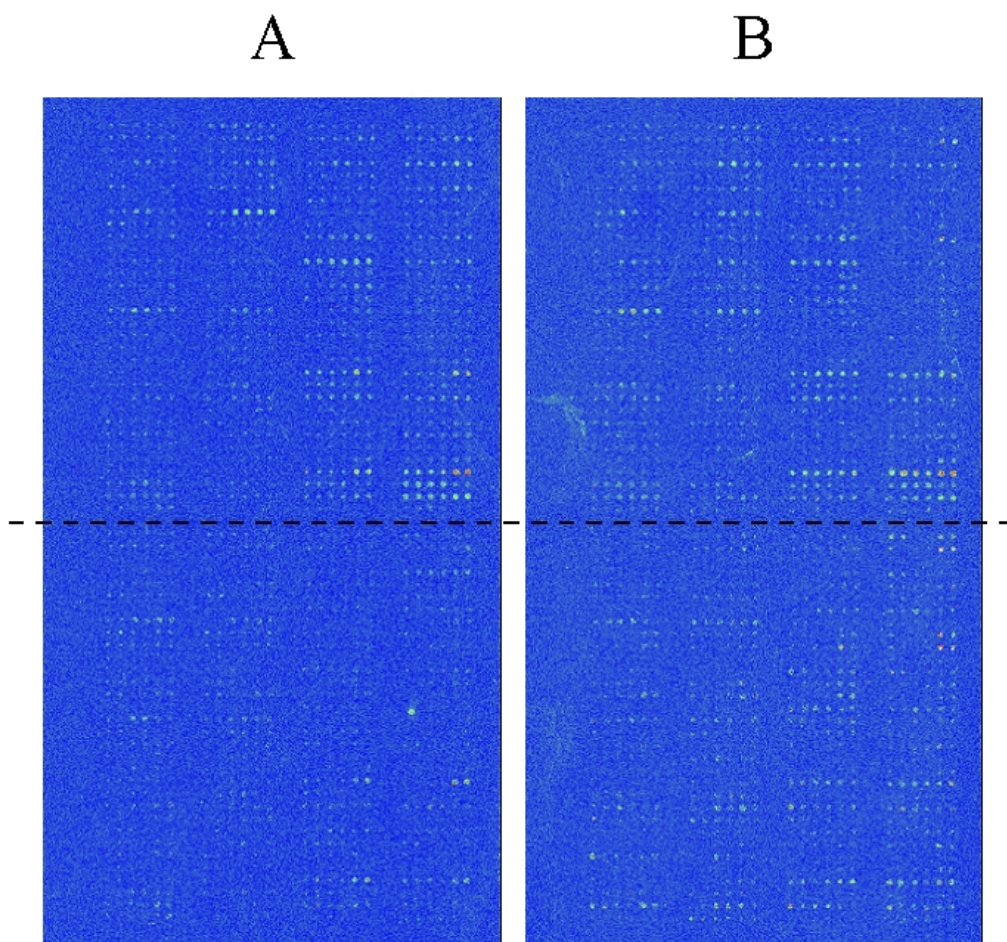


Figure 24: Scan of two microarrays used for the optimisation of the washing procedure. Slide A displays a slide washed with TBS-TT, while slide B shows a slide washed with TBS-T

As a second parameter, the optimal concentration of proteins was determined that was spotted for immobilisation. For evaluation, four proteins were spotted in concentrations of 0.1, 0.05 and 0.02 mg/ml onto epoxy-activated slides. After spotting and post-processing, the proteins were detected by 0.1 $\mu\text{g/ml}$ of monoclonal anti-RGS-His antibodies that were visualised with 1 $\mu\text{g/ml}$ of Cy5-labelled anti-mouse antibodies (Figure 25). The lowest concentration in which all proteins were detected should indicate the minimal concentration of proteins used for scFv screening.

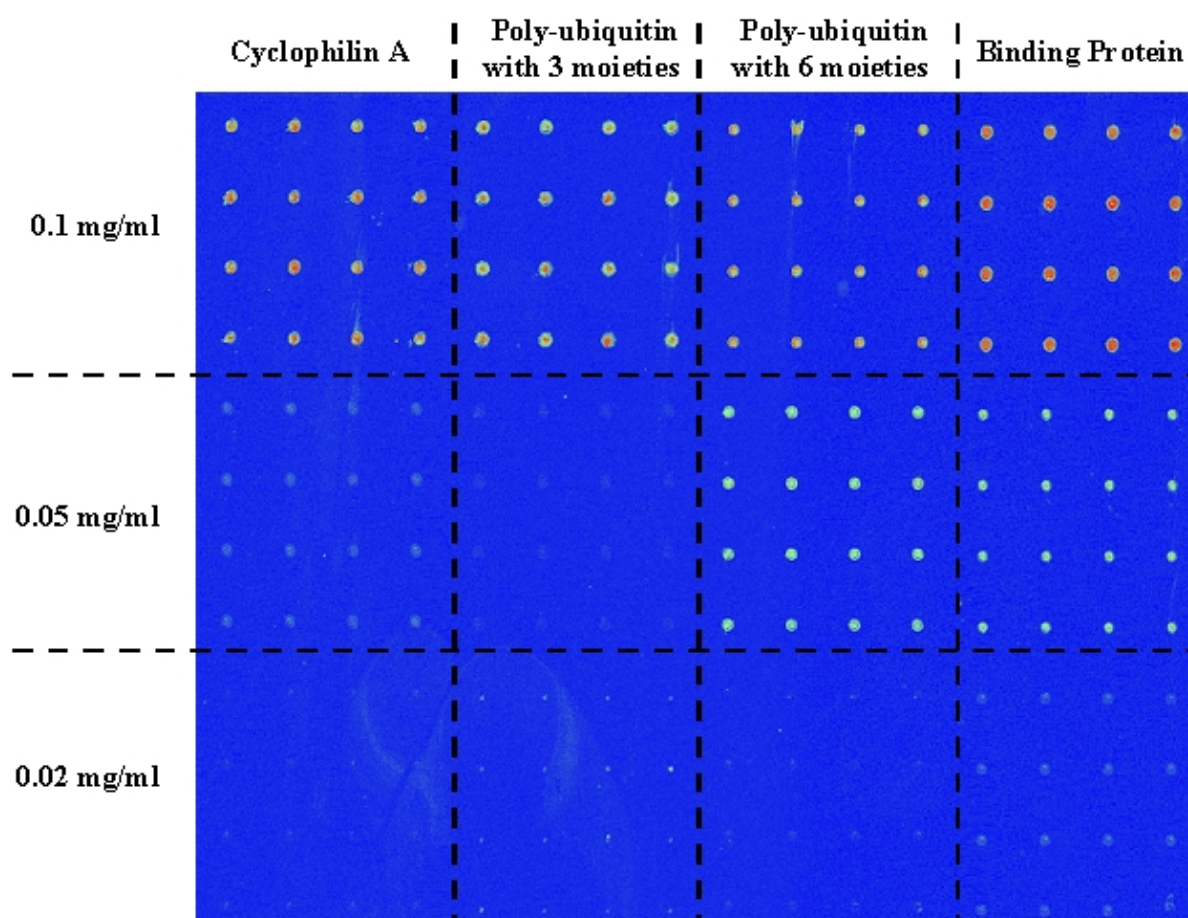


Figure 25: Scan of an epoxy-coated slide with different protein concentrations for determination of the optimal protein concentration for scFv screening

The last parameter that was optimized was the expression strain. Two strains, HB2151 and TG-1 were compared. While TG-1 is the strain that is used in the selection, HB2151 is used for expression of scFv's after selection, since it provides higher yields of scFv's and does not produce scFv-pIII fusions (121). A comparison of both strains expressing the same scFv's against PDLIM1 and CALM2 is shown in Figure 26. 0.1 mg/ml of both antigens were spotted on the top half of epoxy-activated slides, while no protein was spotted on the bottom half of the slide. Unpurified scFv's against both PDLIM1 and CALM2 were spotted onto both, the corresponding antigen in the top half of the slide and on blocked surface on the bottom half. Both slides were treated identically with the exception that slide A contained an array of "guide" spots with two spots in the top left corner and one spot in the bottom right corner of the square covered by each pin. The guide spots consisted of a fluorophore, which was immobilised for orientation purposes.

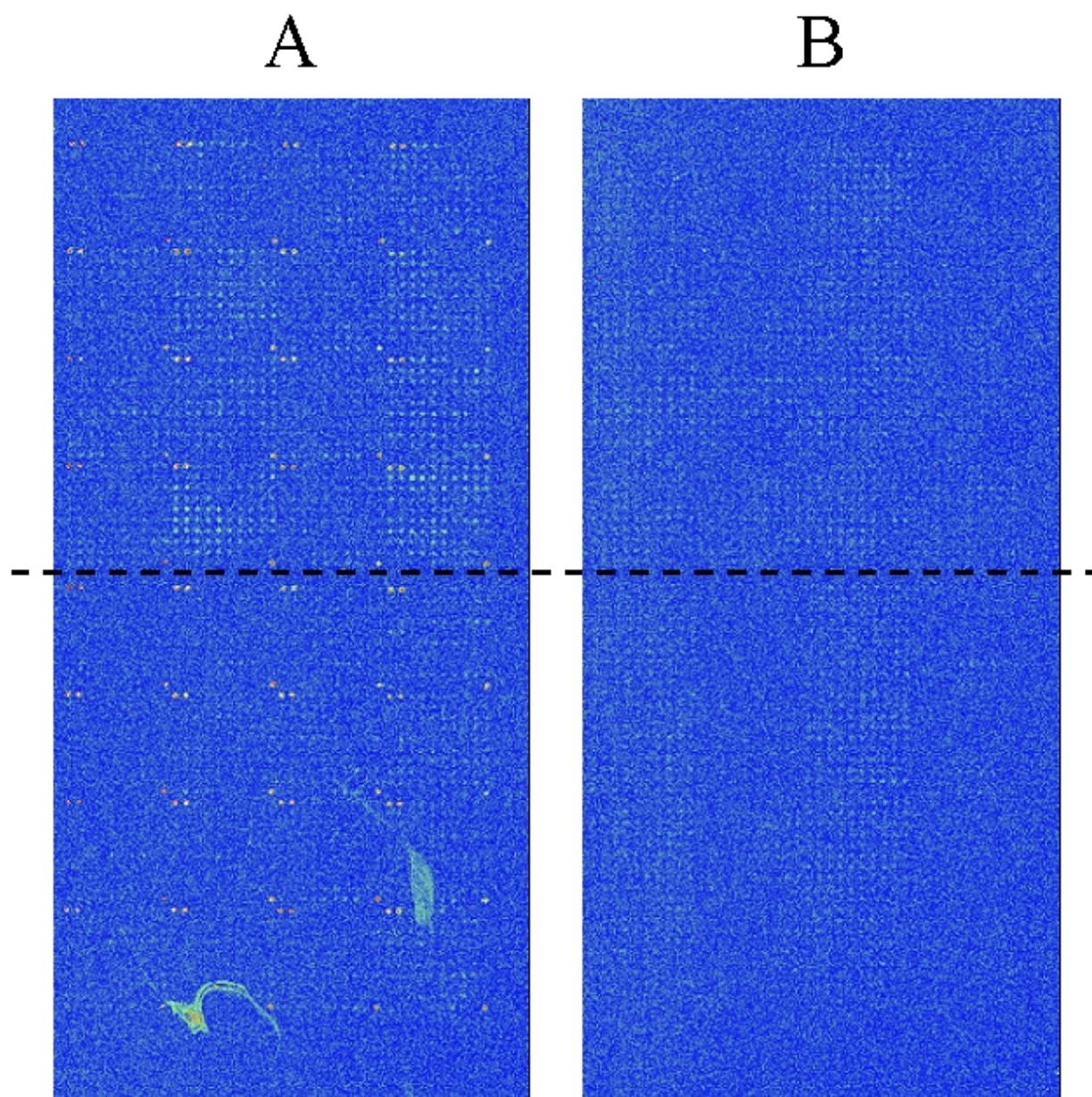


Figure 26: Scan of two slides for comparison of the TG-1 strain (A) and the HB2151 strain (B) for expression of scFv's

5.2.1.4 Enzymatic Assays

Each enzyme requires the optimisation of several parameters to display maximal activity, such as the reaction buffer composition, the incubation time and the substrate concentration. Although the provision of an ideal surface may also be an issue of optimisation, which is dependent on the characteristics of each enzyme, the selection of the surface chemistry was performed for all enzymes using HRP as a model enzyme. Three different coatings were compared, all bearing different properties. While poly-L-lysine provides a positively charged surface, which attracts all negatively charged compounds by electrostatic interactions, polystyrene cell culture slides offer uncharged alkane and alkene groups, which interact with

uncharged hydrophobic groups of proteins by van-der-Waals forces. However, the comparison of different surfaces (122) revealed that the immobilisation capacity of polystyrene slides is rather low. As a third surface, epoxy-coated slides were incubated with BSA to provide a BSA-coated microarray surface, which should prevent direct protein-glass surface and stabilise the enzyme. A comparison of the mean signal intensities of a horseradish peroxidase assay performed on all three surface coatings is shown in Figure 27.

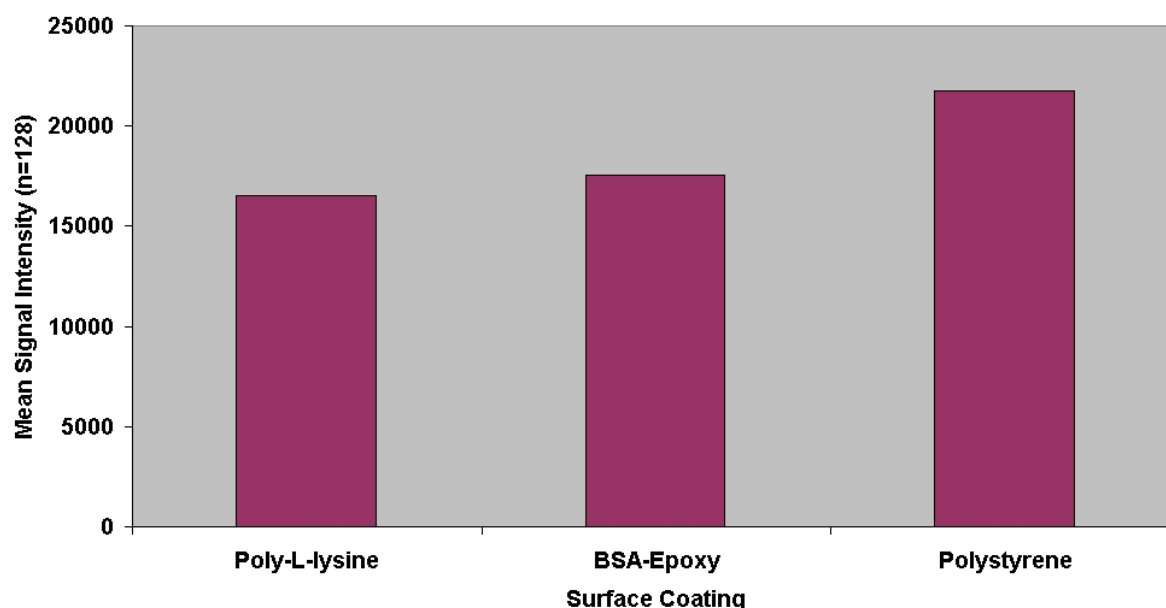


Figure 27: Mean signal intensity versus surface coating for an horseradish peroxidase assay

5.2.2 Application of the Multiple Spotting Technique

5.2.2.1 Immunosorbent Assay

Different assays were performed applying the MIST alone (Figure 28, Figure 29) and in combination with a standard total incubation (Figure 30, Figure 31). All assays were performed by immobilisation of 0.1 mg/ml protein or antibody on the top half of an epoxy-coated slide, while a negative control was performed on the bottom half of the same chip, in which 3% (w/v) non-fat dry milk dissolved in TBS-T was immobilised instead of a binder. In a second spotting step, different concentrations of the respective binding partner were spotted onto both parts of the chip to demonstrate specific binding. The signal intensities of the interactions were calculated by:

$$\frac{\text{Average Signal Intensity}_{\text{Analyte-binder}} - \text{Average Signal Intensity}_{\text{Negative Control}}}{\text{Pin Coefficients}}$$

Diagrams of the calculated signal intensities versus spotted concentration were drawn and the pin coefficients were used to normalize the obtained data.

Figure 28 shows the scan of an antibody microarray assay, in which different amounts of Cy5-labelled HSA ranging from 0.5 to 30 amol per spot were spotted in a second spotting step onto immobilised anti-HSA antibodies in the top half and on blocked surface in the bottom half. Quantification of the signals was performed and an average signal intensity versus spotted concentration diagram with standard deviation error bars was drawn (Figure 29).

Two protein microarray assays were performed, one using monoclonal anti-HSA antibodies ranging from 69.3 to 1.2 amol per spot for detection of HSA (Figure 30) and one using polyclonal anti-fibrinogen ranging from 22 to 0.38 amol per spot for the detection of fibrinogen (Figure 31).

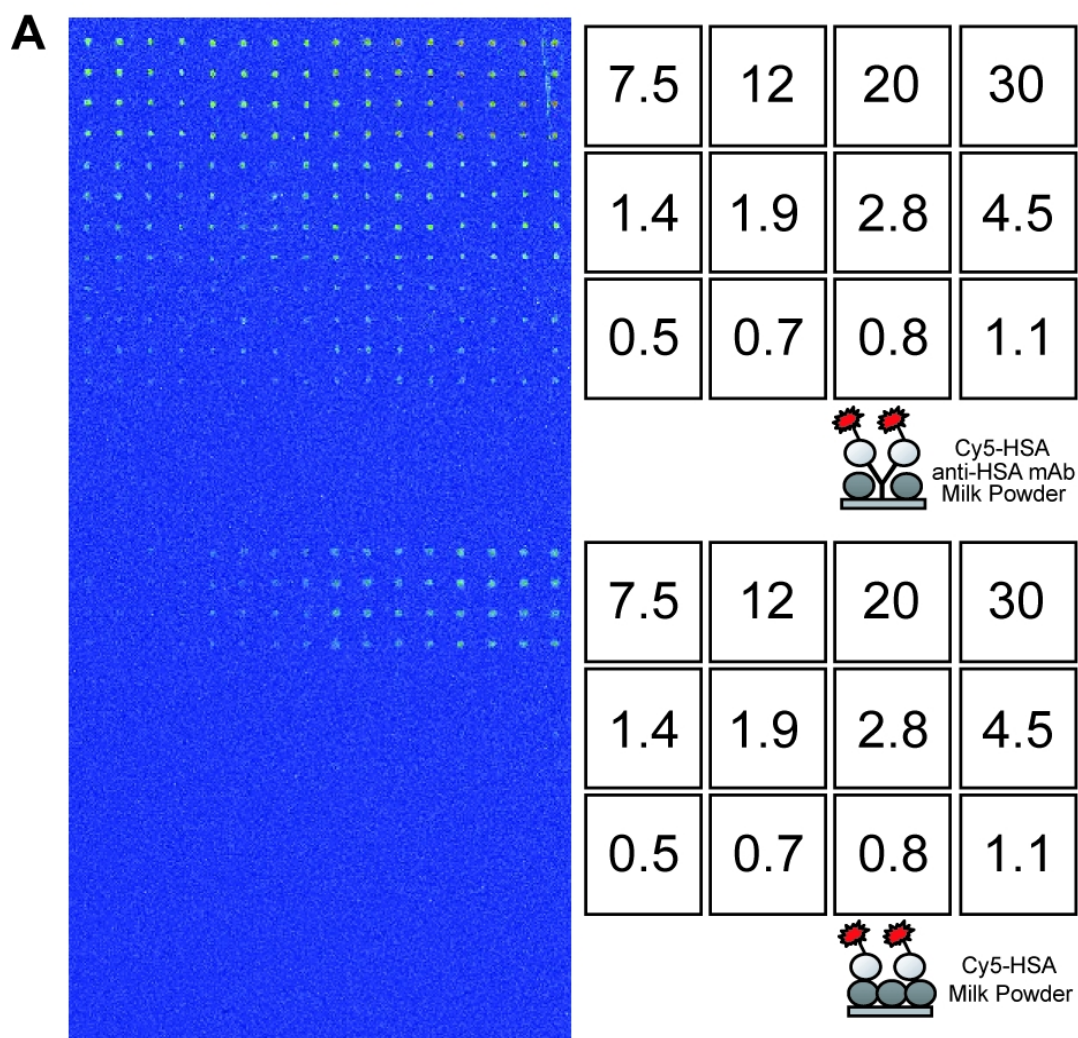


Figure 28: Immunosorbent assay on an antibody microarray using MIST. Left: Scan of an antibody chip. Right: Scheme of the second spotting with Cy5-labelled HSA and illustration of the molecular assembly on the chip. Numbers in squares indicate spotted amount of Cy5-labeled HSA in amol per spot

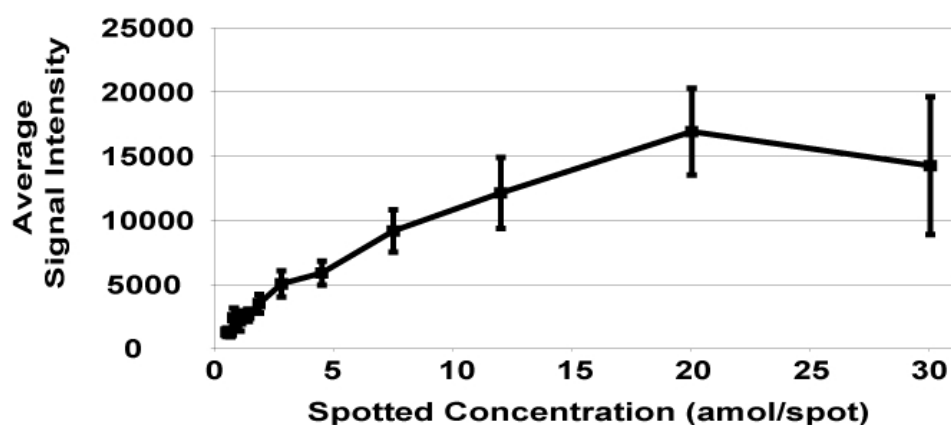


Figure 29: Average signal intensity versus spotted concentration for the microarray shown in Figure 28 with standard deviation error bars

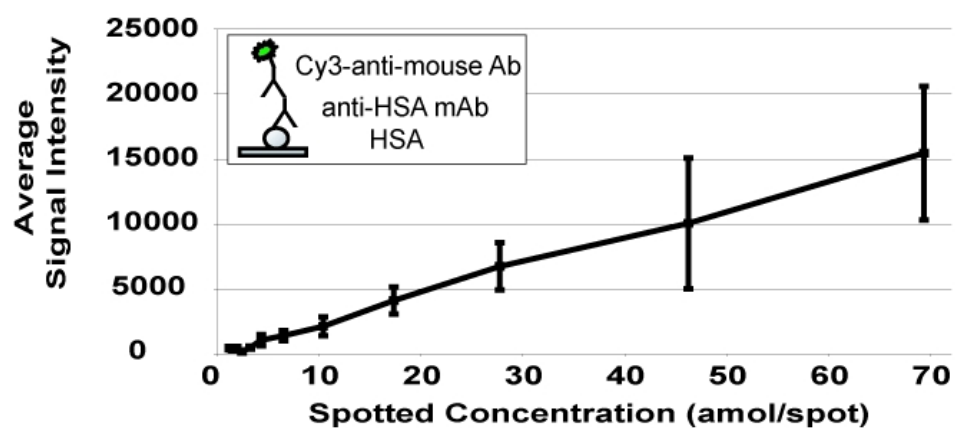


Figure 30: Average signal intensity versus spotted concentration of a protein microarray detected with monoclonal anti-HSA antibodies

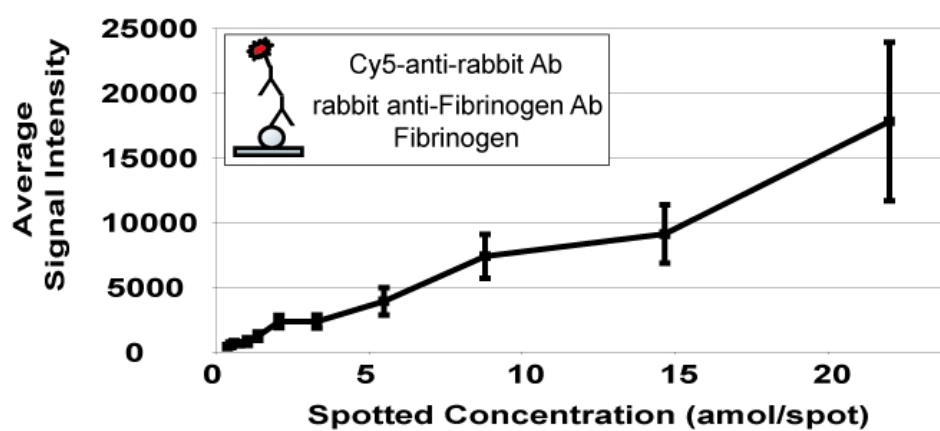


Figure 31: Average signal intensity versus spotted concentration of an protein microarray detected with polyclonal anti-fibrinogen antibodies

To analyse specificity, a multiplex screening approach was conducted on a protein microarray by immobilisation of 90, 181, 451 and 903 amol/spot HSA. In a second spotting step, equimolar concentrations of 10, 21, 42 and 83 amol per spot of polyclonal anti-fibrinogen antibodies and monoclonal anti-HSA antibodies were spotted onto the slides in a perpendicular fashion. Detection of the spotted primary antibodies was performed by a total chip incubation with differently labelled secondary antibodies.

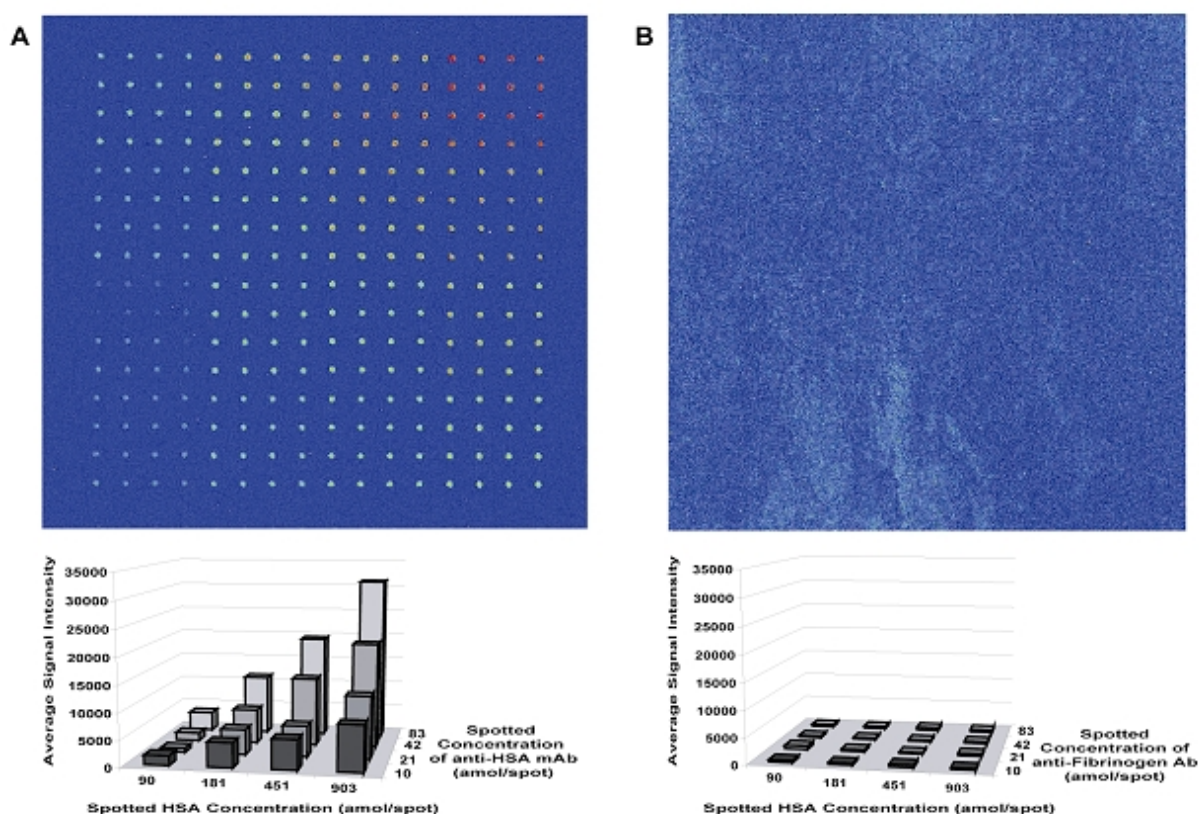


Figure 32: Scan and quantification of spotted monoclonal anti-HSA (A) and polyclonal anti-fibrinogen antibodies (B), which were spotted in equimolar ratio on a protein chip

5.2.2.2 *ScFv Screening Assay*

For application in a scFv screening assay, four proteins, cyclophilin A, poly-ubiquitin, CALM2 and PDLIM1 were expressed and purified under native conditions. Expression and purification was checked on a denaturing SDS-PAGE gel (Figure 33 and Figure 34), which revealed distinct bands in the elution columns. Quantification of the protein concentration was performed by Bradford after exchange of the elution buffer to PBS.

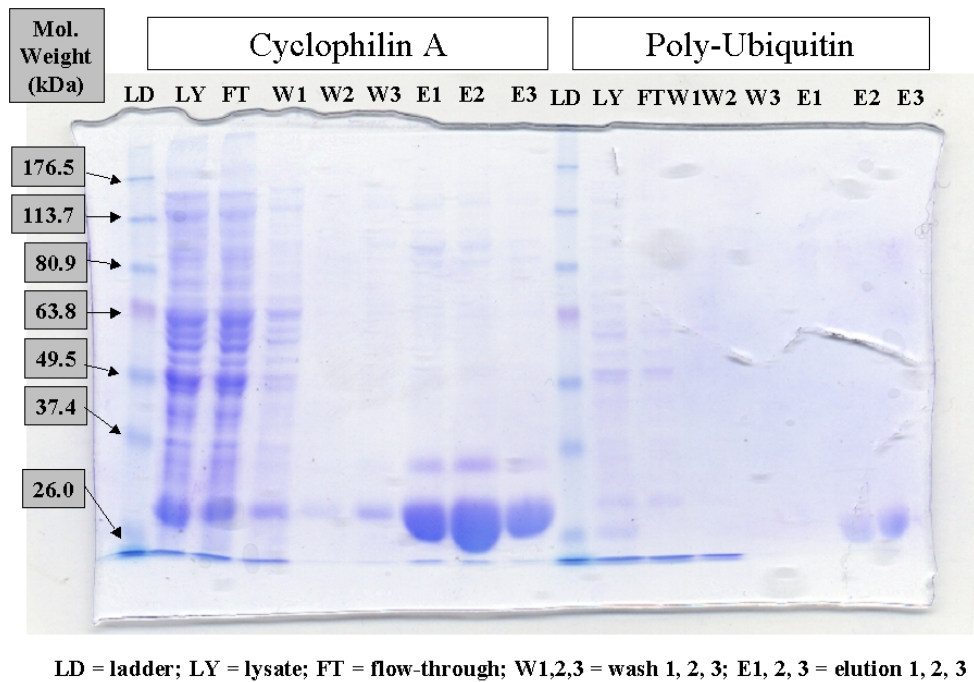


Figure 33: Denaturing SDS-PAGE of cyclophilin A and poly-ubiquitin with three ubiquitin moieties

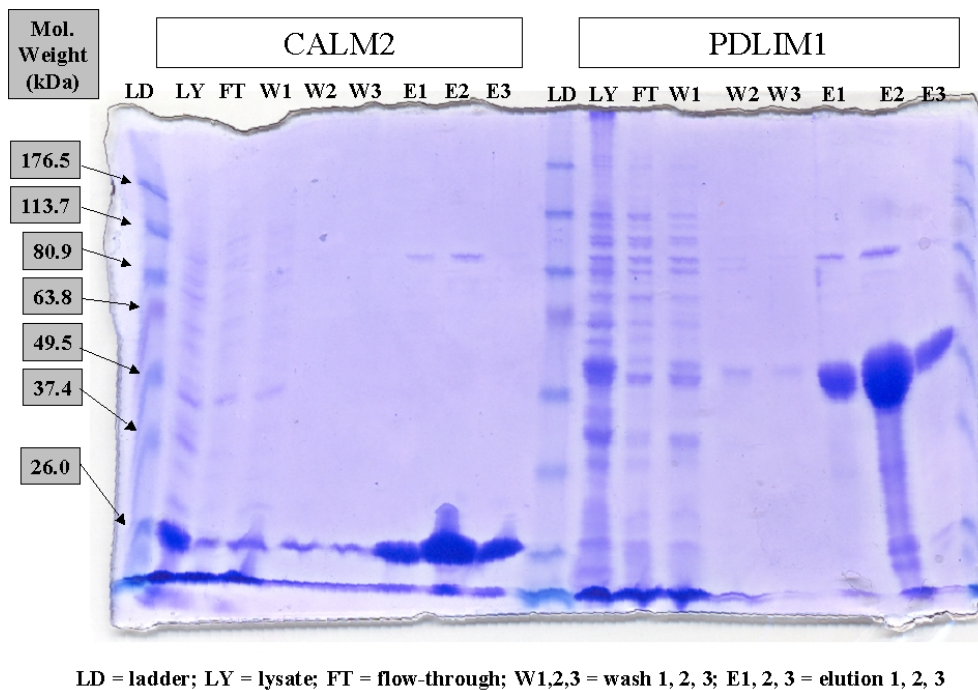


Figure 34: Denaturing SDS-PAGE of CALM2 and PDLIM1

To ensure proper scFv production in TG-1 cells and to assess the detection limits of the new technique in comparison to ELISA, an overnight culture of two monoclonal anti-poly-ubiquitin scFv's was prepared in expression media. A uniform concentration of 0.2 $\mu\text{g/ml}$ poly-ubiquitin was spotted onto epoxy-activated slides, which were blocked after overnight incubation at 4°C. A dilution series of the overnight culture ranging from the original concentration to a 1:10,000 dilution was prepared and spotted in sets of 10 spots per

concentration onto the immobilised poly-ubiquitin. As a negative control, undiluted culture was also spotted onto sections of the slide, which did not contain any poly-ubiquitin, but blocked surface. After incubation with 1 $\mu\text{g/ml}$ Cy5-labelled Protein L, the signals were quantified and the signal intensities of the negative control were subtracted. To allow direct comparison of the data, the same cultures were subjected to ELISA and screened in duplicates. To display the dynamic range of both techniques and allow comparison, the ELISA plates were scanned after 15 minutes and after overnight incubation at room temperature. After analysis and subtraction of the negative control values, two plots of signal intensity/absorption versus dilution were drawn for each clone containing both chip data and ELISA data. One plot was generated with the data of the low intensity scan of the chip and the data from the 15-minute incubation of the ELISA plate (Figure 35) and one plot was drawn from the high intensity scanning and the overnight incubation data (Figure 36).

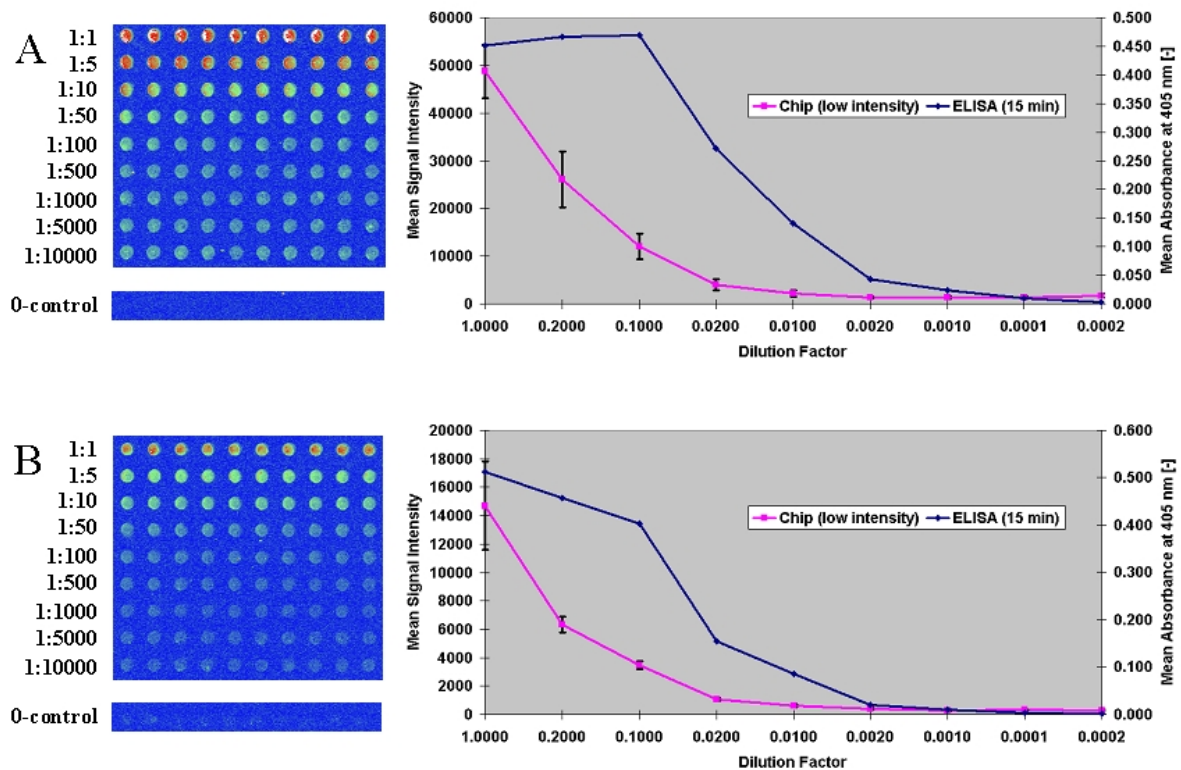


Figure 35: Dilution row of anti-poly-ubiquitin clone from position B1 (A) and E1 (B) using chip data from scanning with low intensities and ELISA data from scanning after 15-minute incubation. Left: Scan of the dilution row as well as the negative control spotted in sets of 10 spots per concentration step. Numbers indicate the dilution. Right: Mean signal intensity and mean absorbance at 405 nm versus dilution factor with standard deviations for the chip data. Since ELISA data was obtained from duplicates, no standard deviations were calculated for the ELISA data

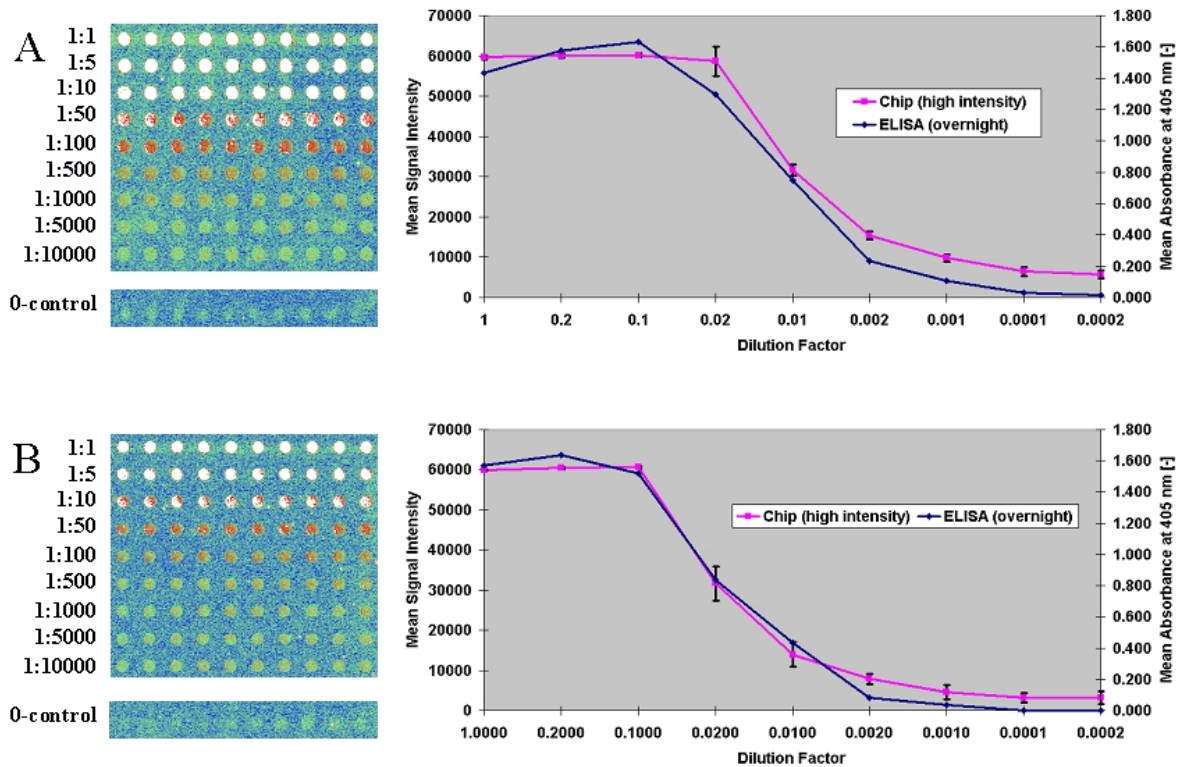


Figure 36: Dilution row of anti-poly-ubiquitin clone from position B1 (A) and E1 (B) using chip data from scanning with high intensities and ELISA data from scanning after overnight incubation. Left: Scan of the dilution row as well as the negative control spotted in sets of 10 spots per concentration step. Numbers indicate the dilution. Right: Mean signal intensity and mean absorbance at 405 nm versus dilution factor with standard deviations for the chip data. Since ELISA data was obtained from duplicates, no standard deviations were calculated for the ELISA data

To assess the feasibility of the technique for the selection of a multitude of recombinant antibody fragments, four sets of 96 monoclonal scFv fragments were screened, all originating from the fourth selection round of an automated phage display selection against targets of varying size. In a first spotting step 0.2 mg/ml of each target protein was spotted onto epoxy-coated slides and the slides were blocked. In a second spotting step, each set of scFv's was spotted in quadruplicate on its respective target and on blocked microarray surface as a negative control. In parallel, the cultures were subjected to an ELISA to allow comparison of the microarray-based technique to traditional ELISA technique. Both approaches were analyzed and the values for the negative controls were subtracted. A scatter plot of microarray data versus ELISA data was generated from all four selections (Figure 37) and two dashed lines were introduced for easy visualization of microarray signal intensities above 1000 and ELISA absorbance values above 0.5. Additionally, graphs for the direct comparison of both

experiments for the 15 best binders were drawn for each protein, to display the capability of the technique to reduce the amount of clones to be screened (Figure 38).

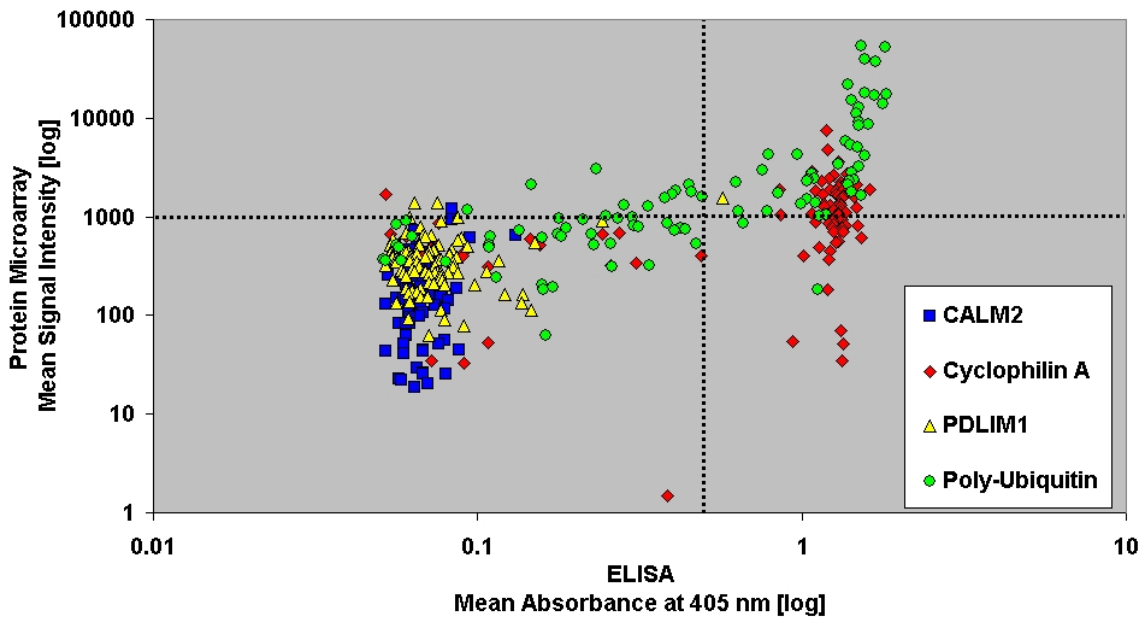
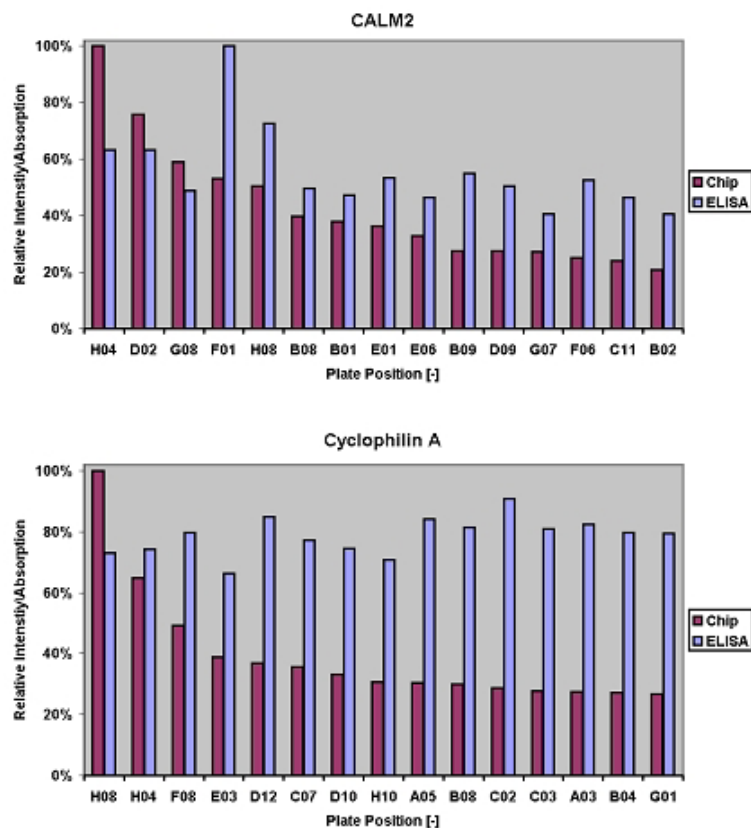


Figure 37: Scatter plot of mean signal intensity of the microarray data versus mean absorbance at 405 nm data from the ELISA. Four selections comprising 96 monoclonal scFv's were screened in parallel. Two dashed lines indicating microarray signal intensities above 1000 and ELISA absorbance values above 0.5 were introduced to allow easy localisation of clear signals



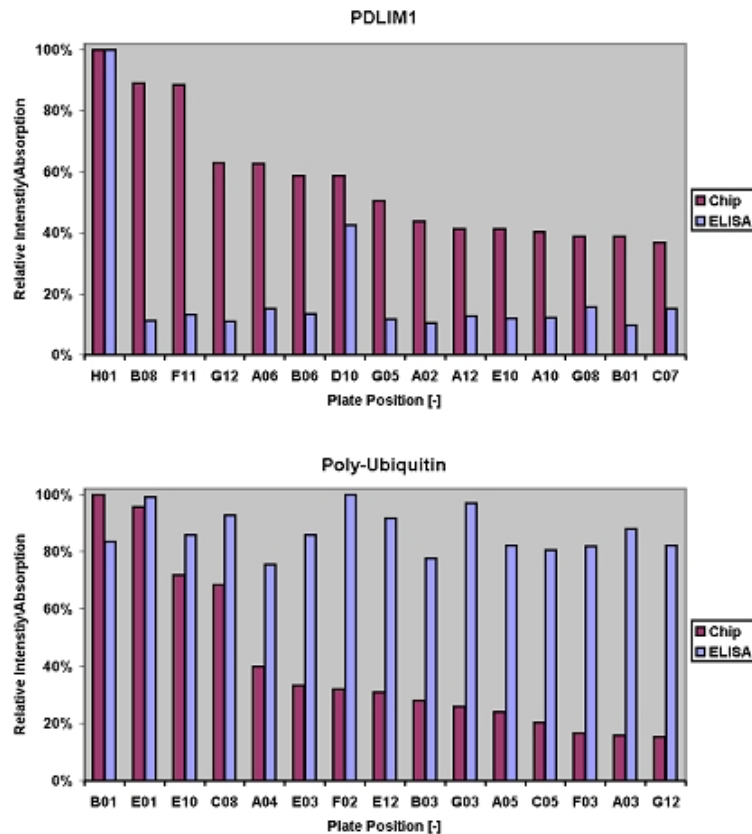


Figure 38: Ordered graphs of relative intensity/absorbance of the best 15 binders for each protein. Ordering was done according to the signal intensity obtained from the microarray data

5.2.2.3 Enzymatic Assays

To demonstrate the principle of enzymatic activity screening on a microarray, different enzymes were tested. The first enzyme tested was the horseradish peroxidase (HRP), which is one of the most commonly used enzymes for ELISA and catalyses oxidation of its substrate by transfer of oxygen from a donor, such as hydrogen peroxide, to the substrate. Since functionality is depended on the heme iron-protoporphyrin IX as a cofactor, activity can be inhibited by addition of sodium azide, which inhibits the attachment of the heme by formation of a meso-azidoporphyrin IX (123). To demonstrate the activity of HRP, an inhibition assay using sodium azide as a specific inhibitor was performed (Figure 39 and Figure 40). The time dependence of enzymatic activity was shown in the same experiment by scanning directly after spotting (designated as 0 h) and after a 2 hour-incubation at 37°C. To display the sensitivity of the reaction, a dilution row of HRP was prepared and deposited in a second spotting step onto the fluorogenic substrate. Again, scanning was performed directly after spotting (0 h) and after 2 hours of incubation at 37°C (Figure 41).

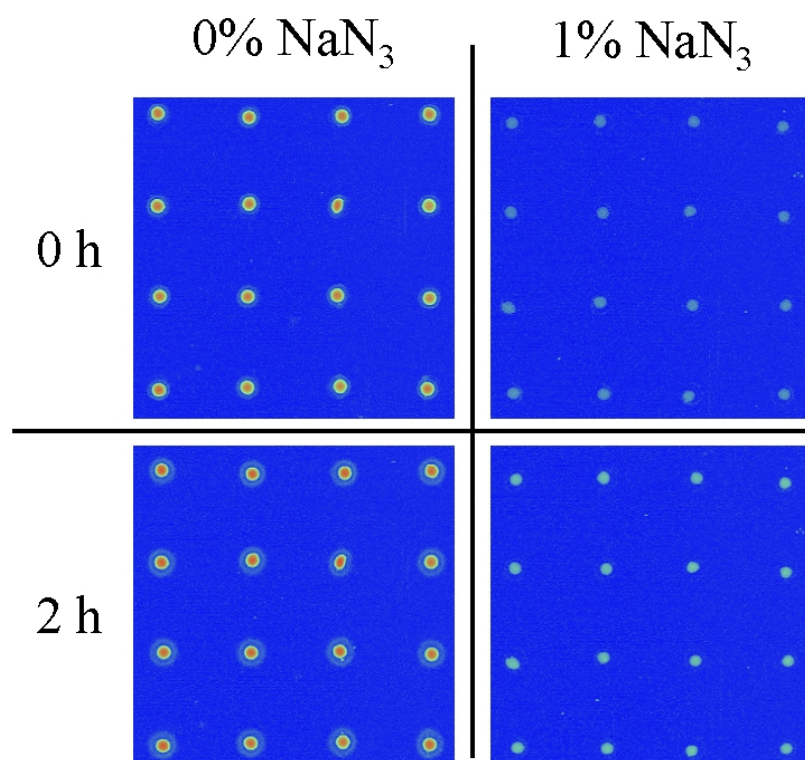


Figure 39: Scans of microarrays for the inhibition assay of HRP using sodium azide as inhibitor

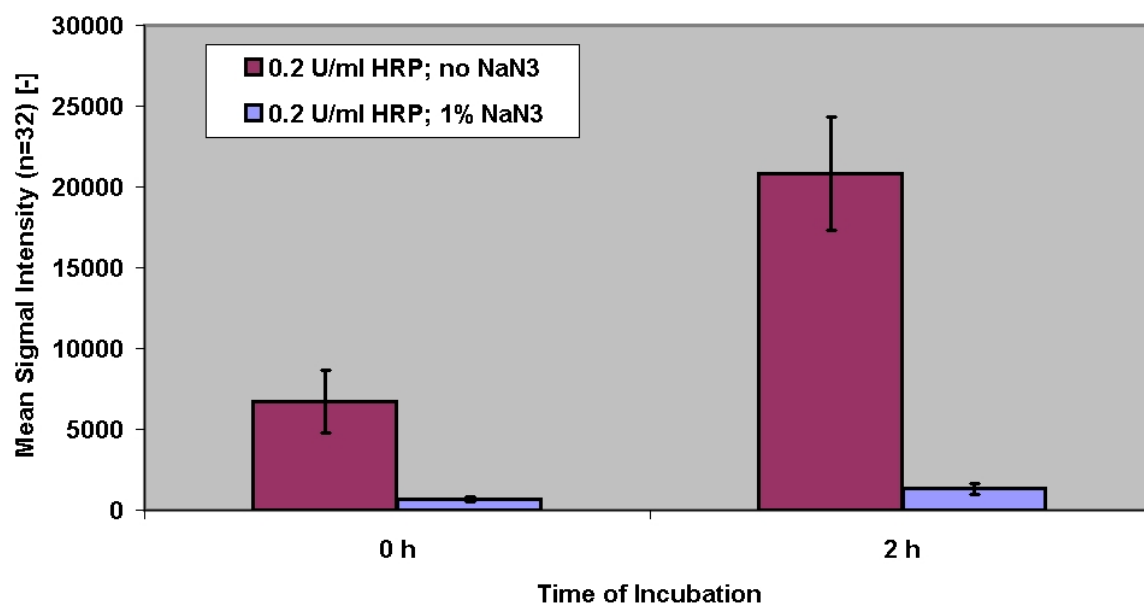


Figure 40: Mean signal intensity versus time of incubation diagram with standard deviation error bars for inhibition assay of HRP. Scanning and analysis was performed without incubation and after 2 hours of incubation

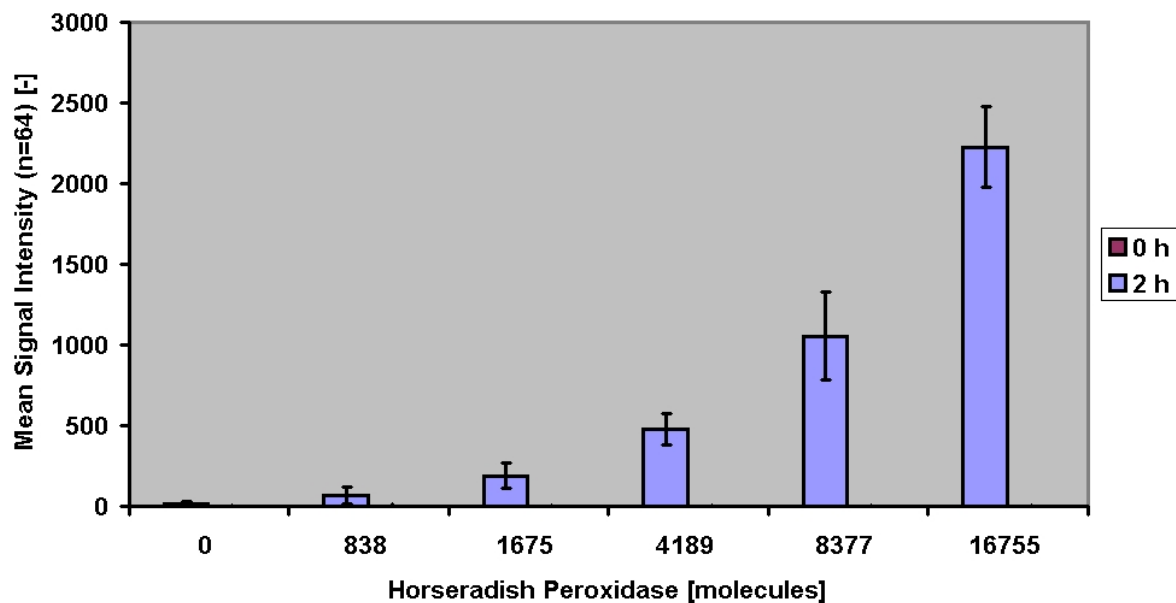


Figure 41: Mean signal intensity versus molecules of HRP diagram with standard deviation error bars for the detection limit assay of HRP. Scanning and analysis was performed without incubation and after 2 hours of incubation

Similar assays to demonstrate applicability of the multiple spotting technique on enzymes were performed using alkaline phosphatase (AP) and β -galactosidase (β -Gal). In contrast to HRP, both enzymes apply different modes of action, with alkaline phosphatase catalysing dephosphorylation and β -galactosidase catalyzing transgalactosidation.

Enzymatic function of AP dependent on divalent cations, which serve as essential activators. Addition of EDTA, which is a well-known chelator of divalent cations, completely abolishes all alkaline phosphatase activity (124). β -Galactosidase catalyses hydrolysis of terminal, non-reducing β -D-galactose residues in β -D-galactosides. Phenethyl β -D-thiogalactoside (PETG) is a non-hydrolysable analogue of β -D-galactose and is commonly used as a selective and reversible inhibitor of β -galactosidase (52, 125, 126). To demonstrate the functionality of both enzymes, AP and β -Gal were subjected to an assay of inhibition (Figure 42 and Figure 44). Moreover a dilution row assay was performed for determination of the detection limits of both enzymes with and without incubation (Figure 43 and Figure 45).

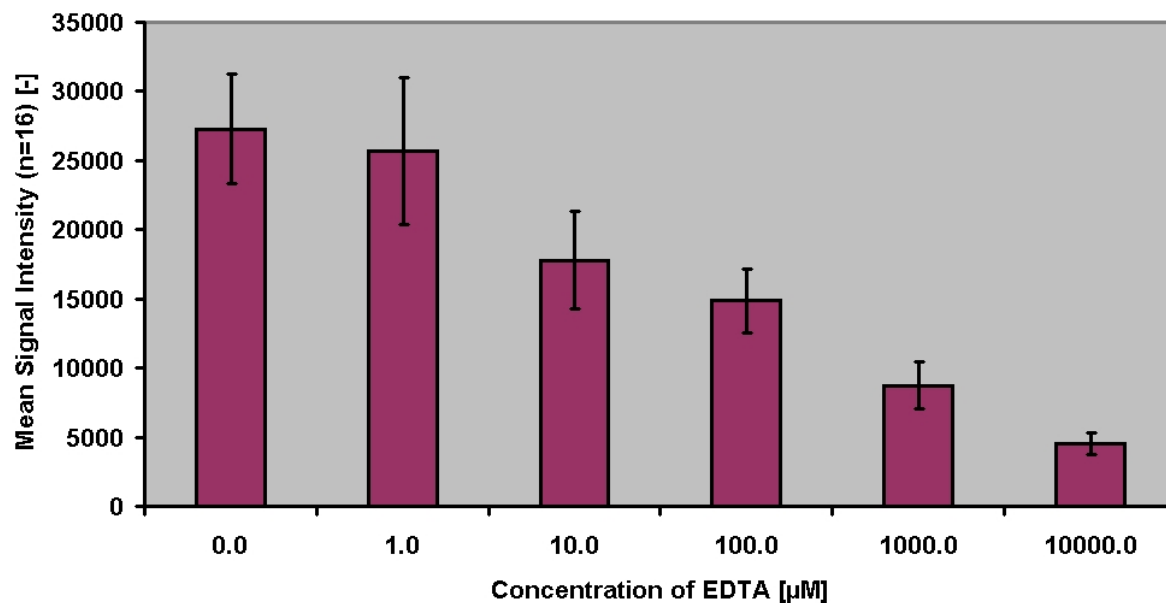


Figure 42: Mean signal intensity versus concentration of EDTA diagram with standard deviation error bars for the inhibition assay of AP. Scanning and analysis was performed without incubation

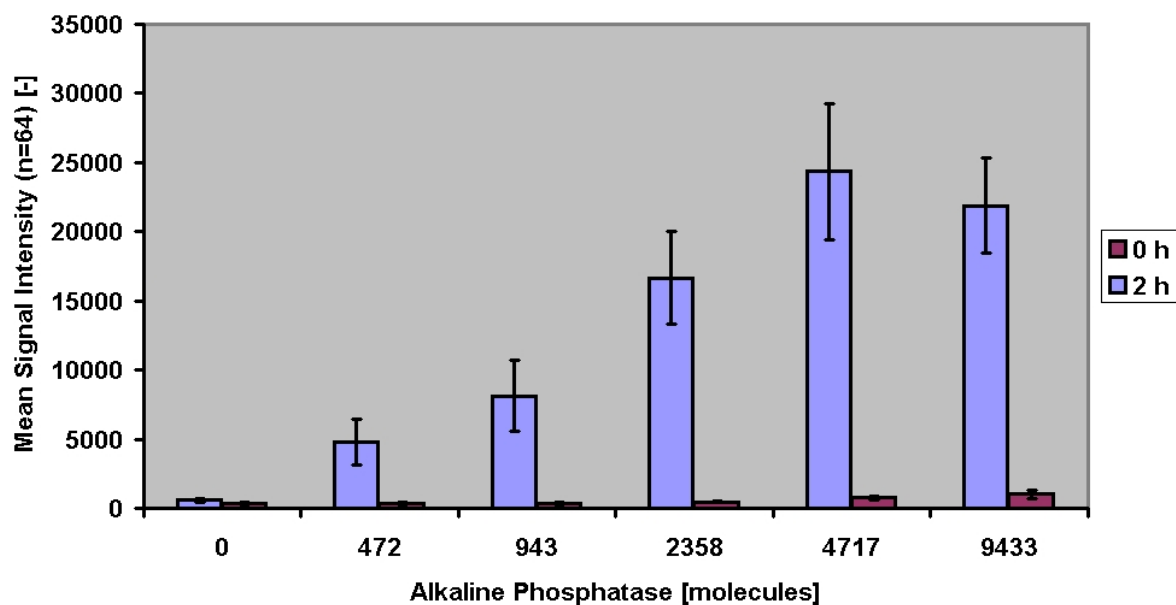


Figure 43: Mean signal intensity versus molecules of AP diagram with standard deviation error bars for the detection limit assay. Scanning and analysis was performed without incubation and after 2 hours of incubation

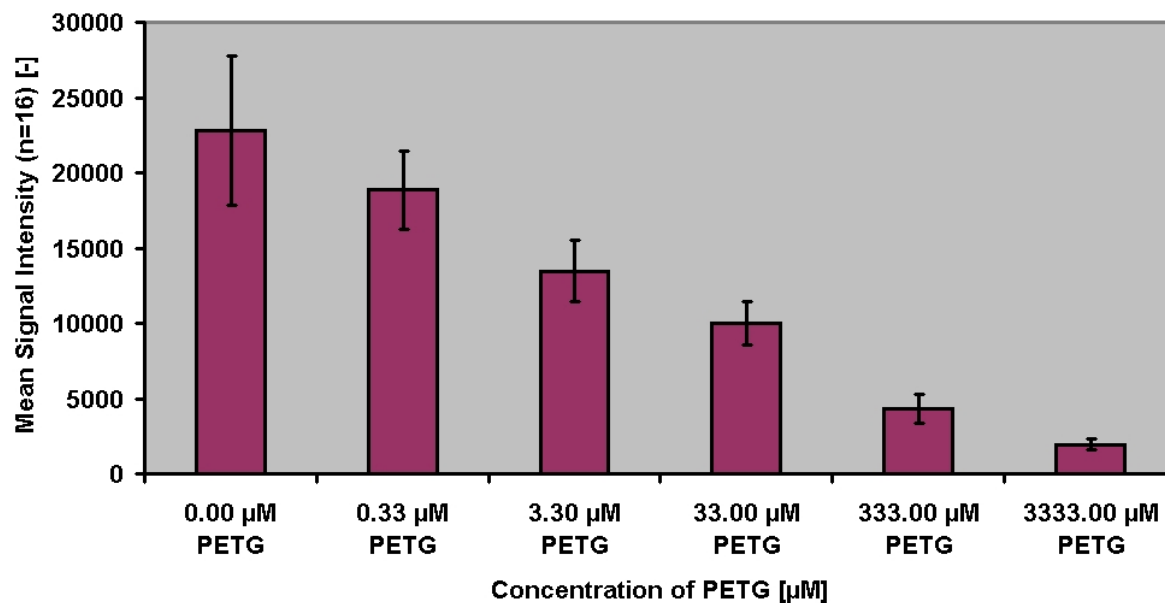


Figure 44: Mean signal intensity versus concentration of PETG diagram with standard deviation error bars for inhibition assay of β -galactosidase. Scanning and analysis was performed without incubation

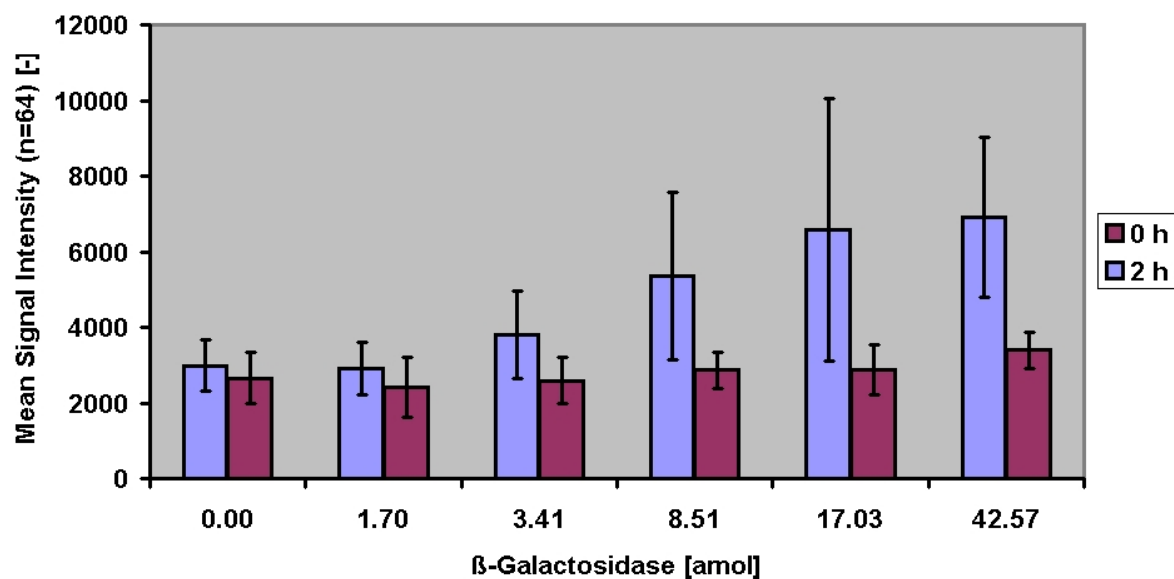


Figure 45: Mean signal intensity versus moles of β -galactosidase diagram with standard deviation error bars for the detection limit assay. Scanning and analysis was performed without incubation and after 2 hours of incubation

Cathepsin D was also tested on microarrays to demonstrate applicability of the multiple spotting technique to more sensitive enzymes with medicinal relevance. Cathepsin D is an acid protease, belonging to the peptidase family A1. It is suggested to play a role in the pathogenesis of sporadic Alzheimer's disease (127) and in the process of tumour invasion and

metastasis of different types of cancer (128, 129). Moreover, measurement of cathepsin D activity can serve as a prognostic marker in breast cancer (130).

A dilution row assay with concentration steps ranging from 4013 to 0 amol was performed and scanned directly after spotting and after a 1-hour incubation at 37°C (Figure 46).

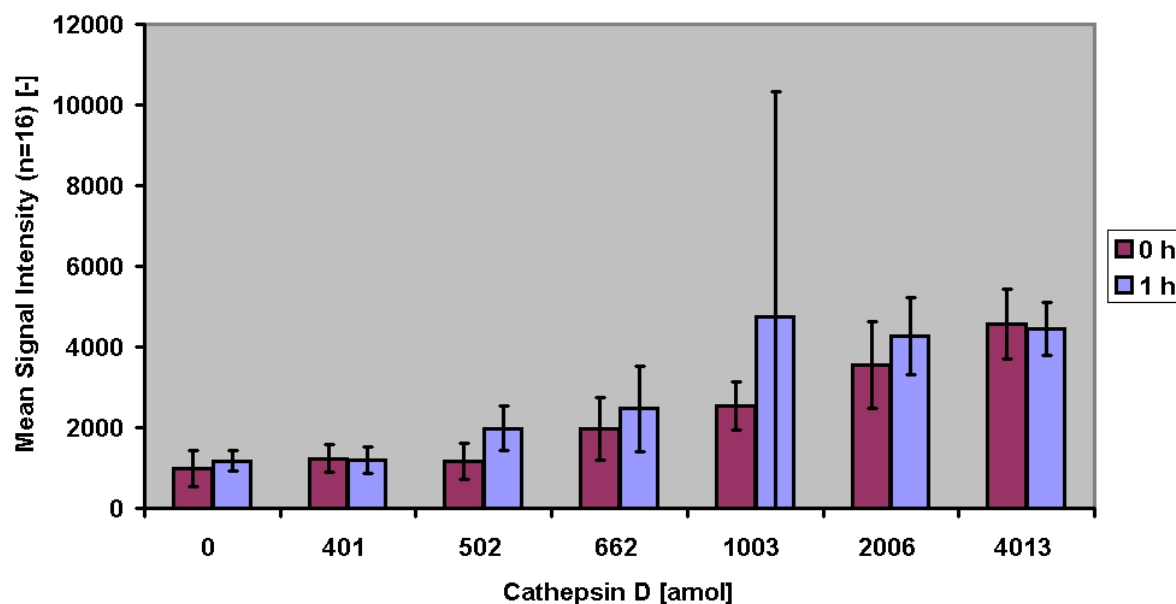


Figure 46: Mean signal intensity versus moles of cathepsin D diagram with standard deviation error bars for the detection limit assay of cathepsin D. Scanning and analysis was performed without incubation and after 1 hour of incubation

To test the possibility of signal amplification, with an AP-conjugated secondary antibody, a dilution row of anti-HSA antibodies was immobilised and detected by either a fluorescently labelled secondary antibody (direct label) or via signal amplification with an AP conjugated secondary antibody (Figure 47).

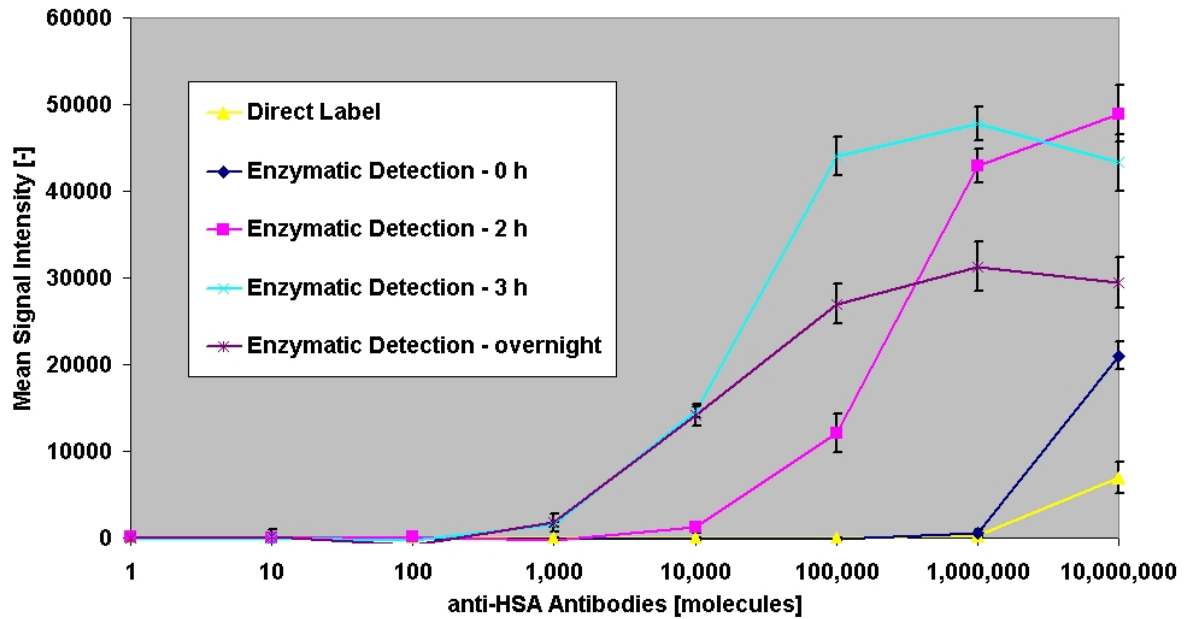


Figure 47: Diagram of mean signal intensity versus anti-HSA antibodies for the enzymatic signal amplification

5.3 Fibrinogenolysis Assay by Substrate Capture

Fibrinogen was spotted at concentrations of 5 mg/ml, 0.5 mg/ml and 0.05 mg/ml from top to bottom onto polyacrylamide slides that were preincubated with PBS. For control of specificity 3 mg/ml GAPDH and 0.5 mg/ml HSA were immobilised as well as 1 mg/ml Cy3-labelled fibrinogen and 3.29 mg/ml polyclonal anti-fibrinogen antibodies for control of labelling and presence of Cy3-labelled fibrinogen. Finally 0.1 mg/ml thrombin was spotted onto the surface for control of unspecific binding of Cy3-labelled fibrinogen to thrombin. The chip was incubated with 2.5 U/ml (1 μ g/ml) thrombin dissolved in 2% (w/v) non-fat dry milk dissolved in TBS-T, washed, incubated with 10 μ g/ml Cy3-labelled fibrinogen and washed again (Figure 48). A chip bearing the same immobilised components was processed in parallel with the exception that no incubation with thrombin was performed (Figure 49).

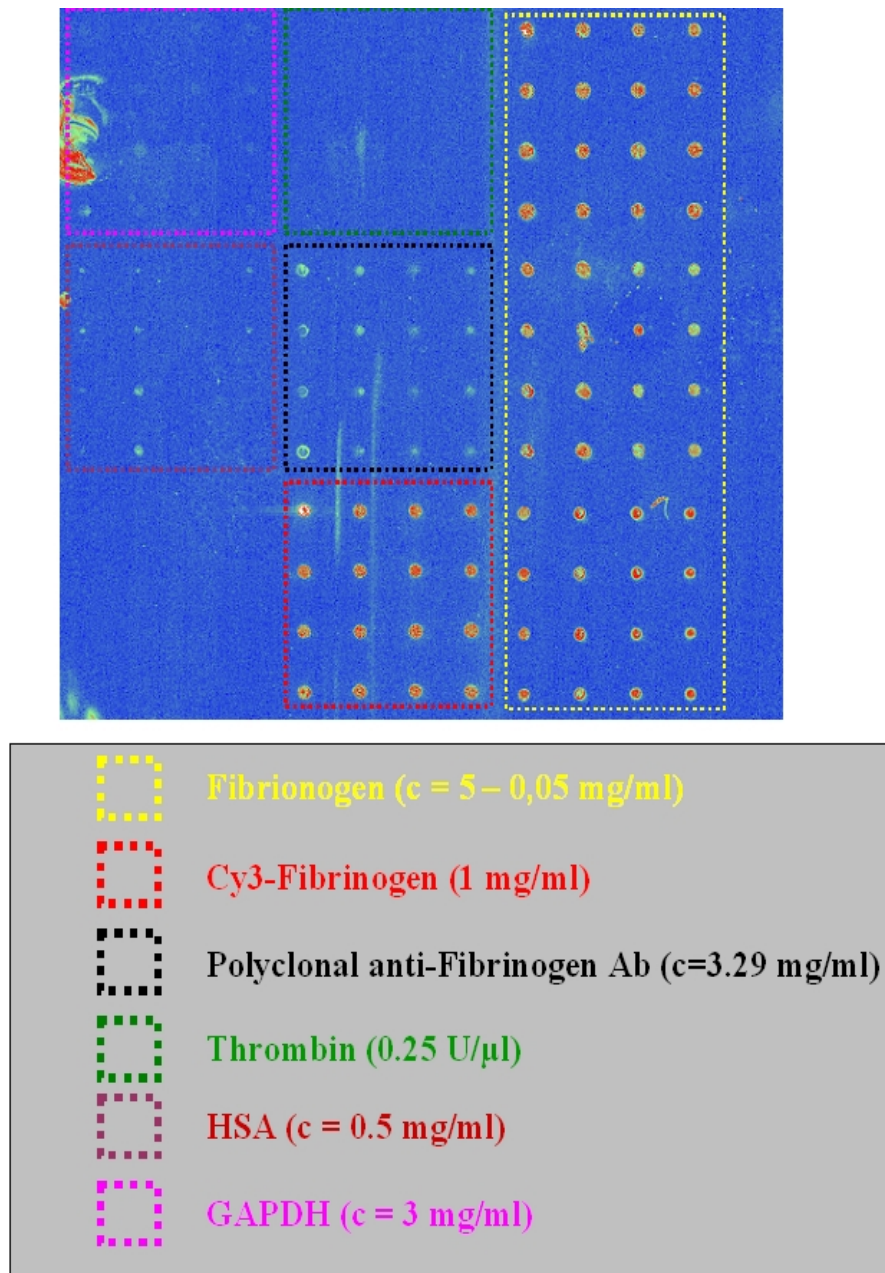


Figure 48: Scan of protein chip incubated with thrombin

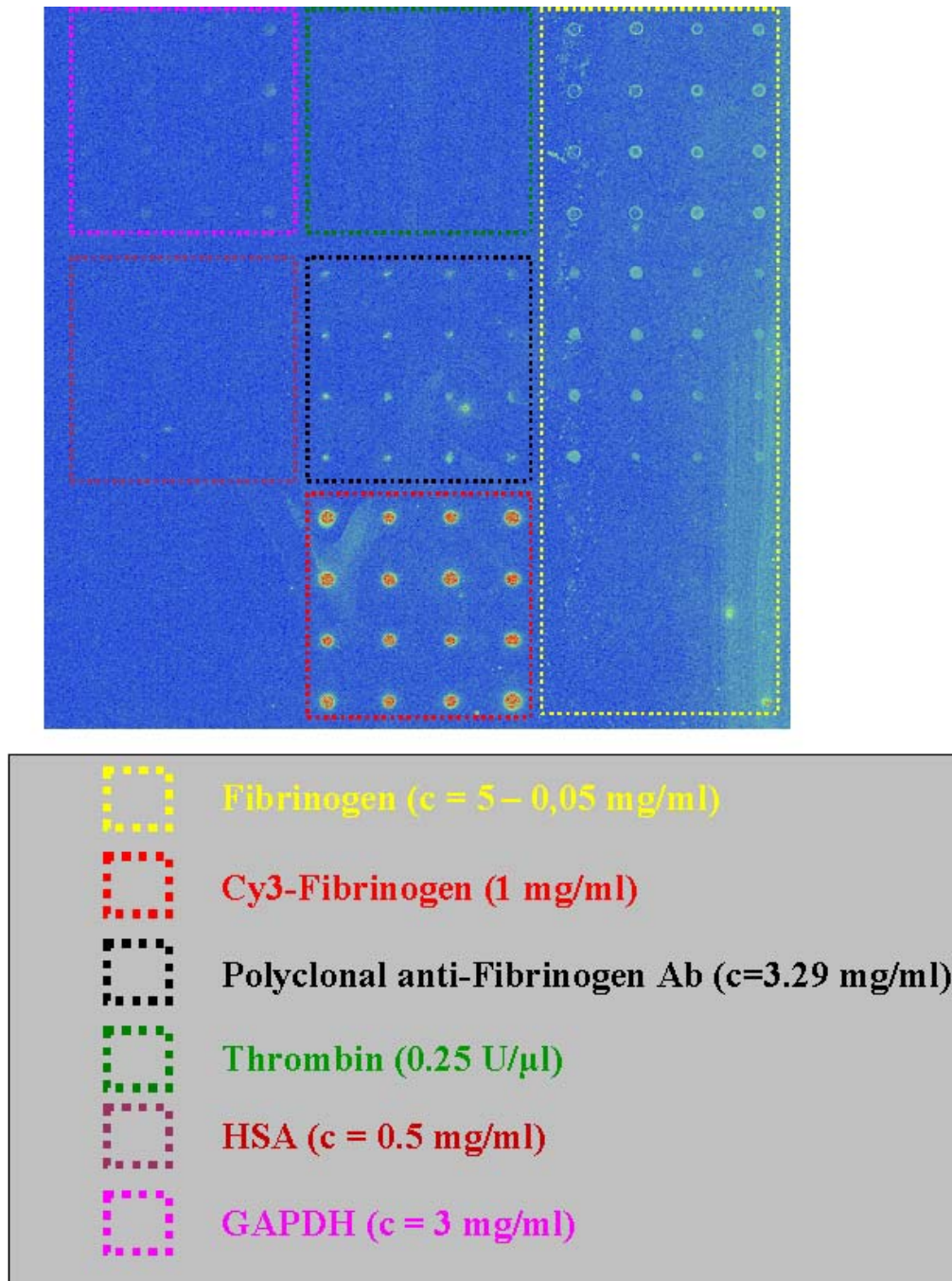


Figure 49: Scan of protein chip incubated without thrombin

To sets of 16 spots of immobilised substance each, were quantified and the mean value as well as the standard deviation were calculated. Normalisation of microarrays from both experiments was performed by setting the signals of Cy3-labelled fibrinogen to 100%. A graph indicating the relative signal intensities versus immobilised substances was drawn (Figure 50).

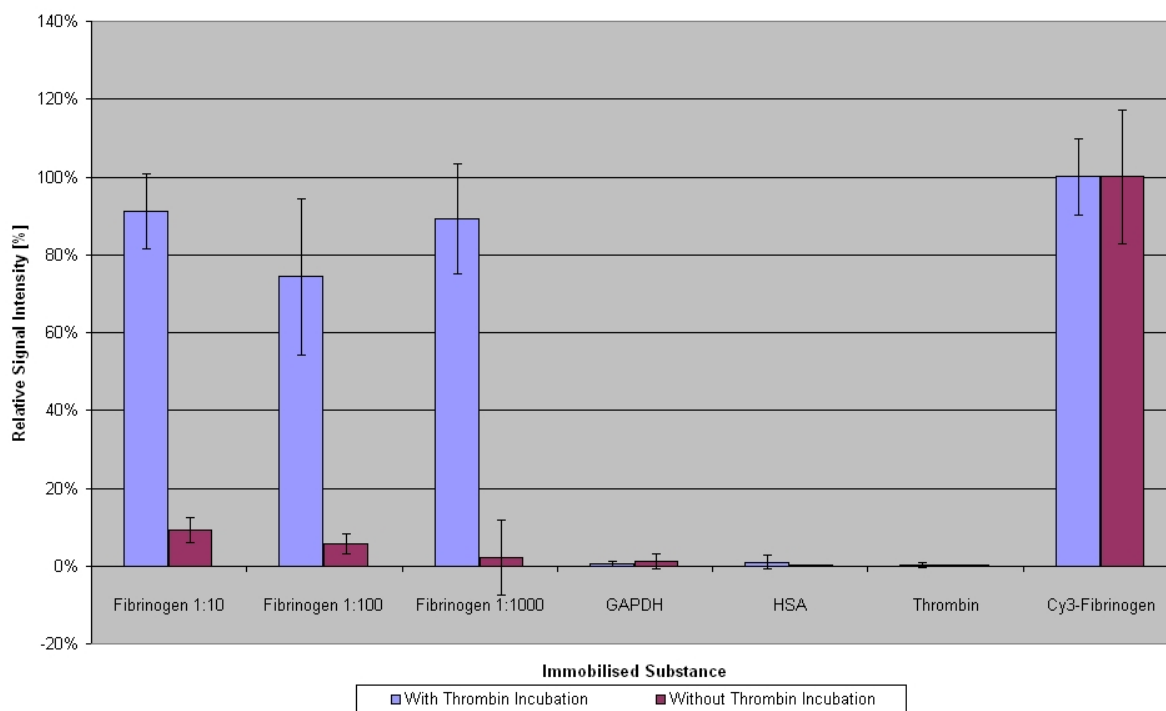


Figure 50: Diagram of relative signal intensity versus immobilised component of slides with and without thrombin incubation

An inhibitor assay using the specific and potent thrombin inhibitor Z-D-Phe-Pro-methoxypropylboroglycinepinane diol ester (ZPPD) ($K_i = 7$ nM) (131, 132) was performed using the multiple spotting technique. In a first spotting step 2 mg/ml fibrinogen was spotted onto polyacrylamide slides that were preincubated with PBS, while 5 mg/ml inhibitor was applied in a second spotting step before the chip was incubated with 0.625 U/ml thrombin and 10 μ g/ml Cy3-labelled fibrinogen (Figure 51 and Figure 52).

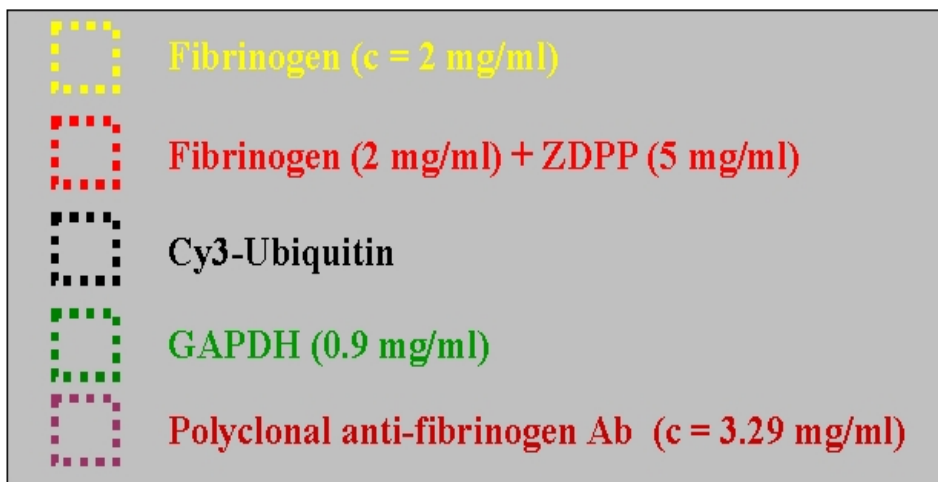
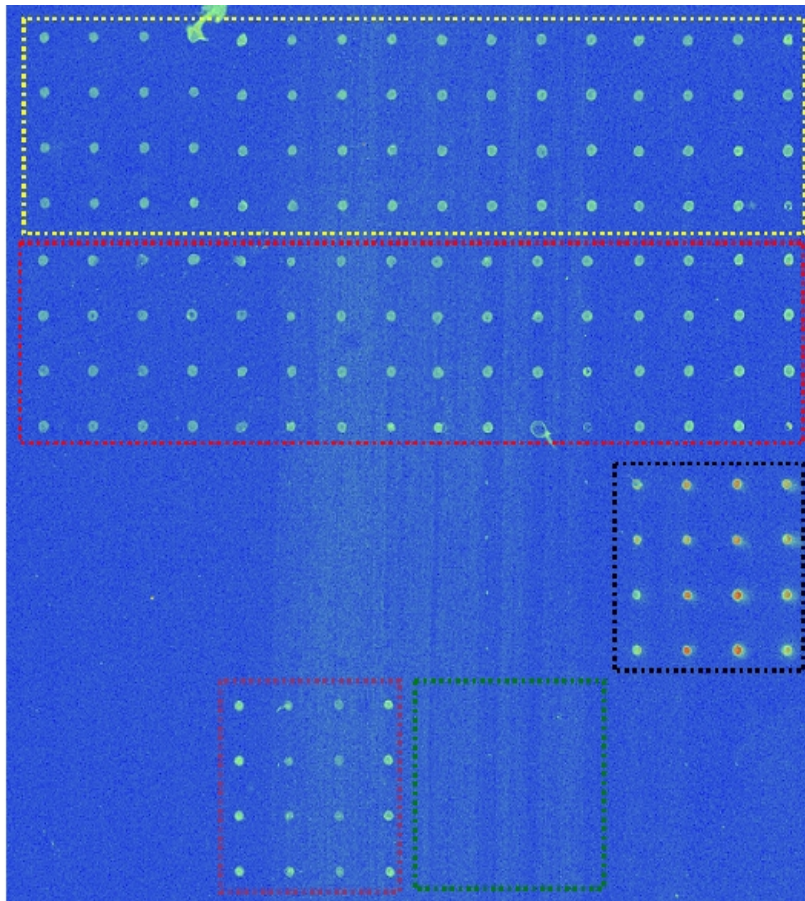


Figure 51: Scan of protein chip with ZDPP applied using MIST

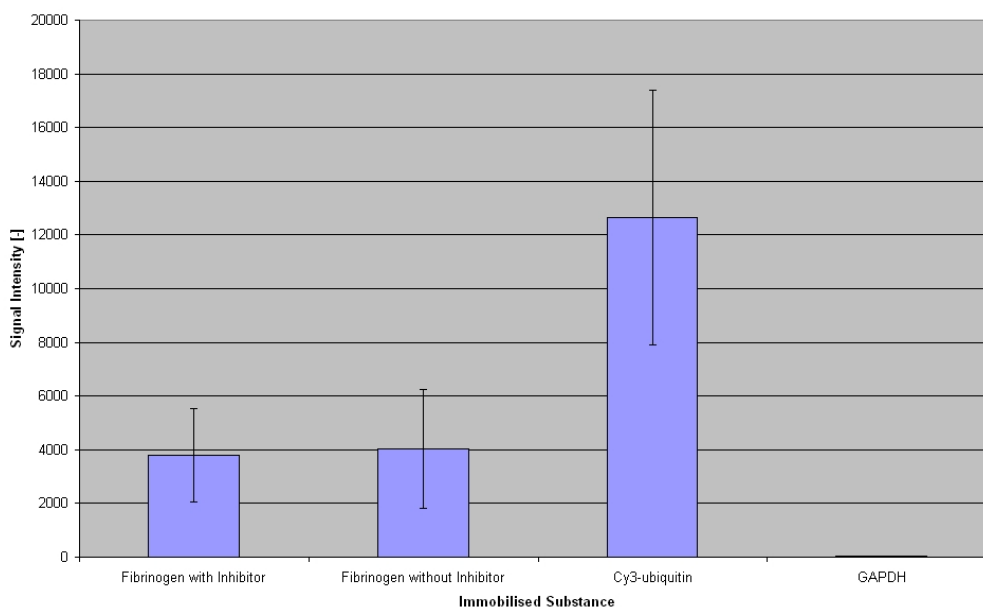


Figure 52: Diagram of signal intensity versus immobilised substance for thrombin inhibitor assay

Additionally, inhibition assays were performed in a 50 μ l-batch using ZPPD and a protease inhibitor cocktail, which both did not show any inhibition of clot formation (data not shown).

5.4 Protein Expression and Analysis in Nanowell Arrays

Two proteins, green fluorescent protein (GFP) and β -galactosidase, were expressed using a cell-free coupled transcription and translation system. The monomeric, active GFP has a unique chromophore formed by spontaneous cyclisation and subsequent oxidation enabling fluorescent detection (133). β -galactosidase consists of four identical subunits of 116.3 kDa forming a 465 kDa protein. The active β -galactosidase hydrolyses sequentially its non-fluorescent substrate fluorescein digalactoside (FDG) to fluorescein monogalactoside and then to highly fluorescent fluorescein, which can be detected at wavelength of 535 nm.

5.4.1 Expression in 50 μ l-Batch

To ensure proper expression, both proteins were expressed *in vitro* using standard transcription and translation mix. GFP was also expressed using a ten-fold prediluted transcription and translation mix. Fluorescent spectra of GFP (Figure 53) and β -galactosidase-processed FDG (Figure 54) were recorded with an excitation wavelength of 474 nm to ensure proper folding of the proteins.

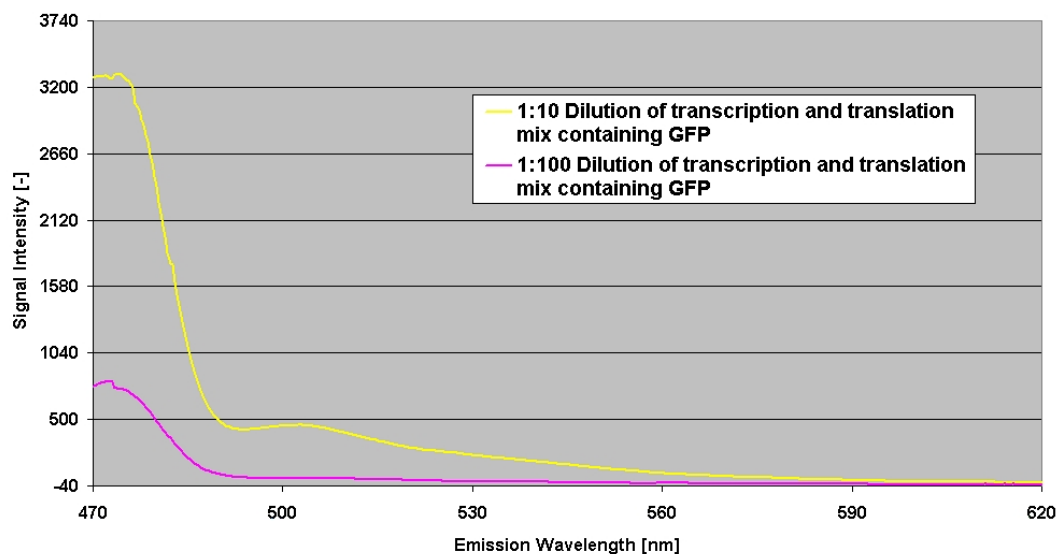


Figure 53: Emission spectra of two dilutions of transcription and translation mix containing GFP

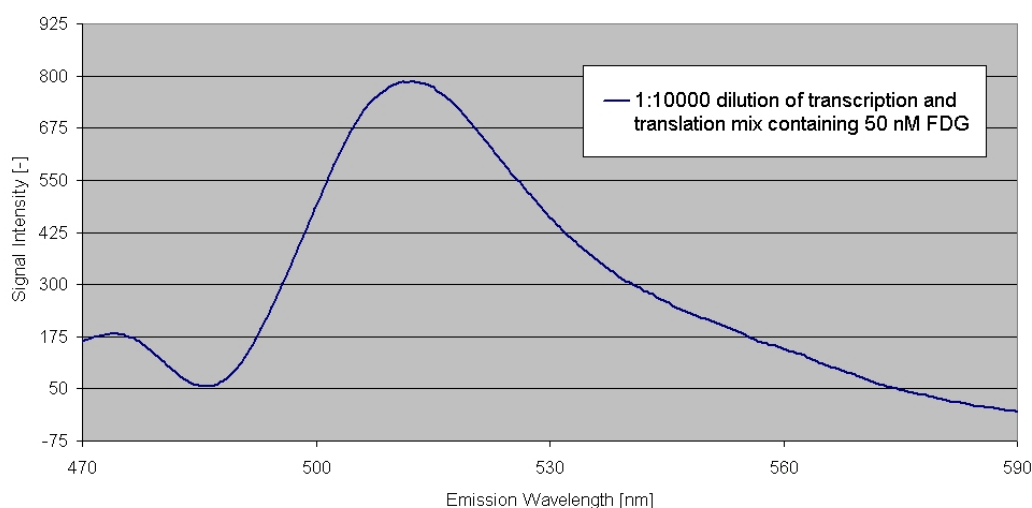


Figure 54: Emission spectra of transcription and translation mix containing β -galactosidase and 50 nM FDG

5.4.2 Detection in Nanowells

Two dilutions of expressed GFP derived from both, undiluted as well as the prediluted 50 μ l-batch, were prepared and different volumes were transferred in duplicates into nanowells. The samples were overlaid with mineral oil to avoid evaporation, and scanned with an excitation of 488 nm and an emission of 535 nm, using a highly sensitive laser scanner (Figure 55 and Figure 56).

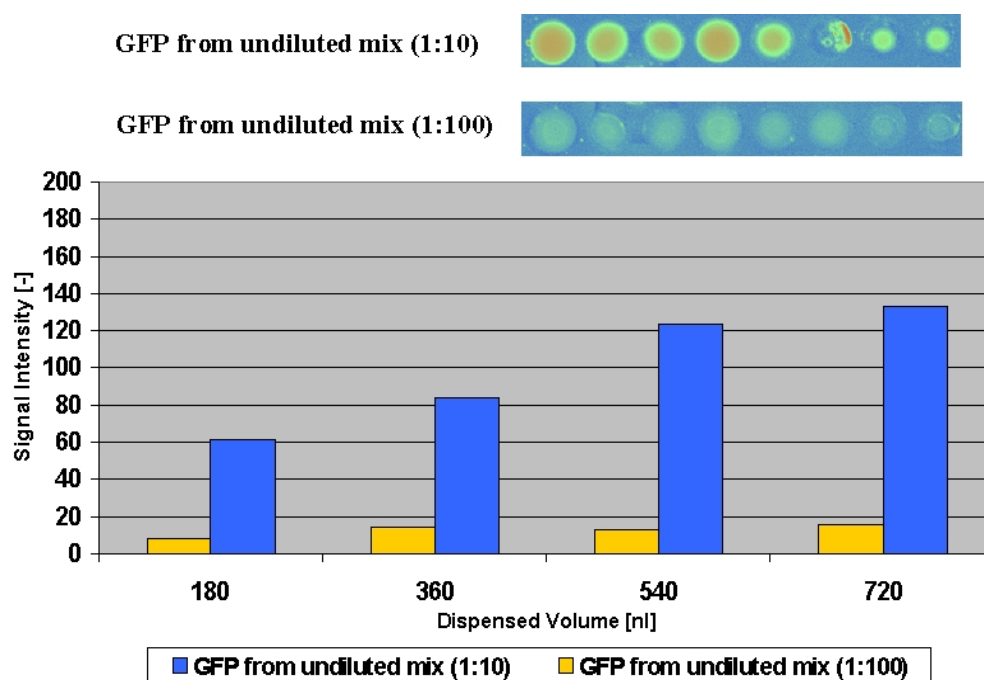


Figure 55: Scan of nanowells and diagram of signal intensity versus dispensed volume for two dilutions of an undiluted cell-free expression mix containing GFP

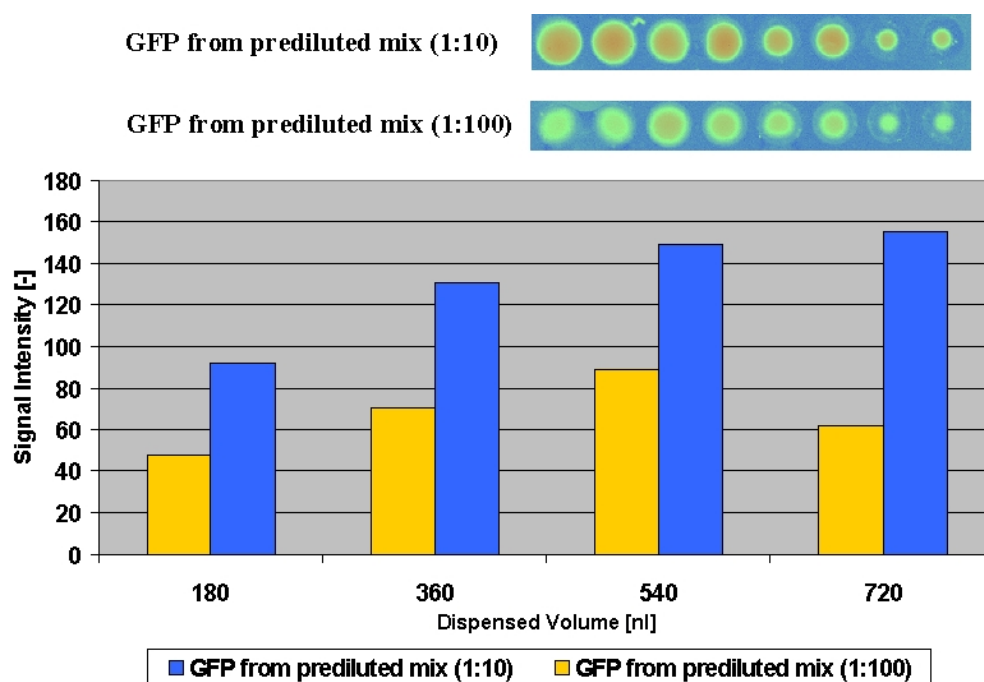


Figure 56: Scan of nanowells and diagram of signal intensity versus dispensed volume of two dilutions of a pre-diluted cell-free expression mix containing GFP

A dilution of the cell-free expression system containing β -galactosidase was prepared and different volumes ranging from 180 - 720 nl were dispensed in duplicates into the nanowells, onto pre-dispensed 180 nl of 5 mM FDG (Figure 57).

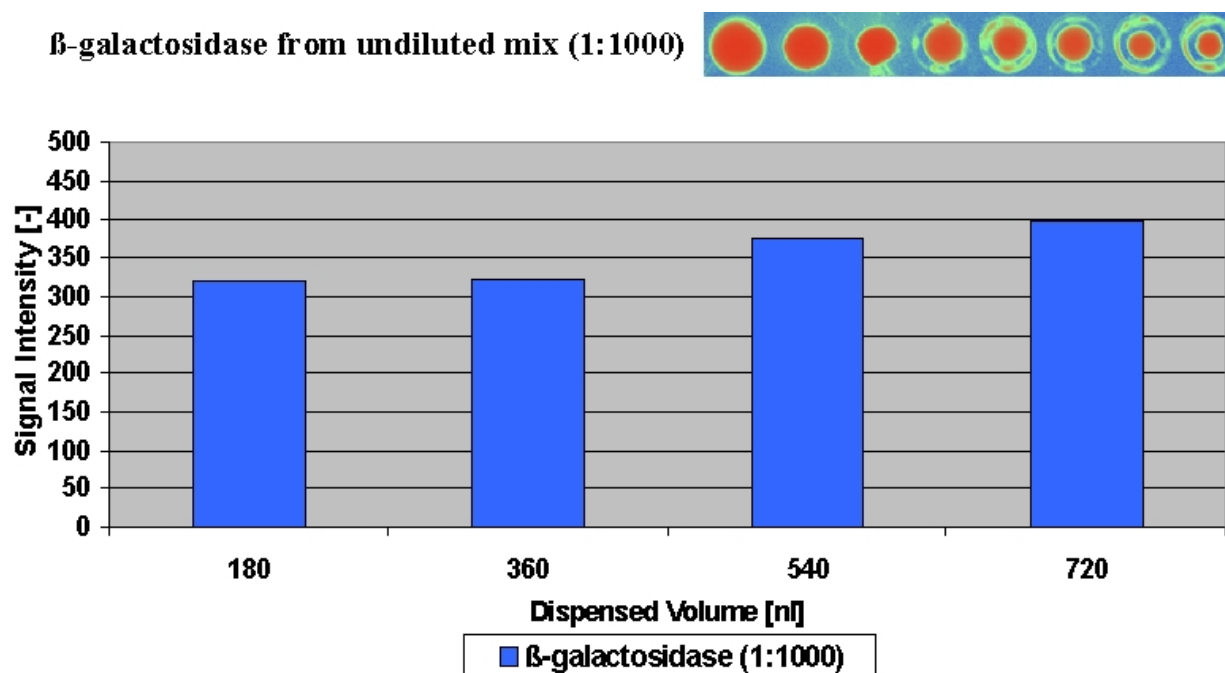


Figure 57: Scan of nanowells and diagram of signal intensity versus dispensed volume for a dilution of an undiluted cell-free expression mix containing β -galactosidase

5.4.3 Cell-free Transcription and Translation in Nanowells

Batches of cell-free transcription and translation mix were prepared and plasmid DNA carrying the coding sequences of GFP and β -galactosidase were added. For control two batches of both expressions were prepared, one with P_{T7} -GFP-DNA, one lacking DNA. Prior to incubation, all samples were transferred in volumes ranging from 0.1 μ l – 1 μ l into nanowells and were overlaid with mineral oil avoiding evaporation. After incubation at 30°C, duplicates of FDG ranging from 0.2 μ l of 5 μ M substrate were added into wells containing expressed β -galactosidase. The nanowell plates were scanned with an excitation of 488 nm, read out at 535 nm, and mean signal intensity versus dispensed volume diagrams were drawn (Figure 58 and Figure 59).

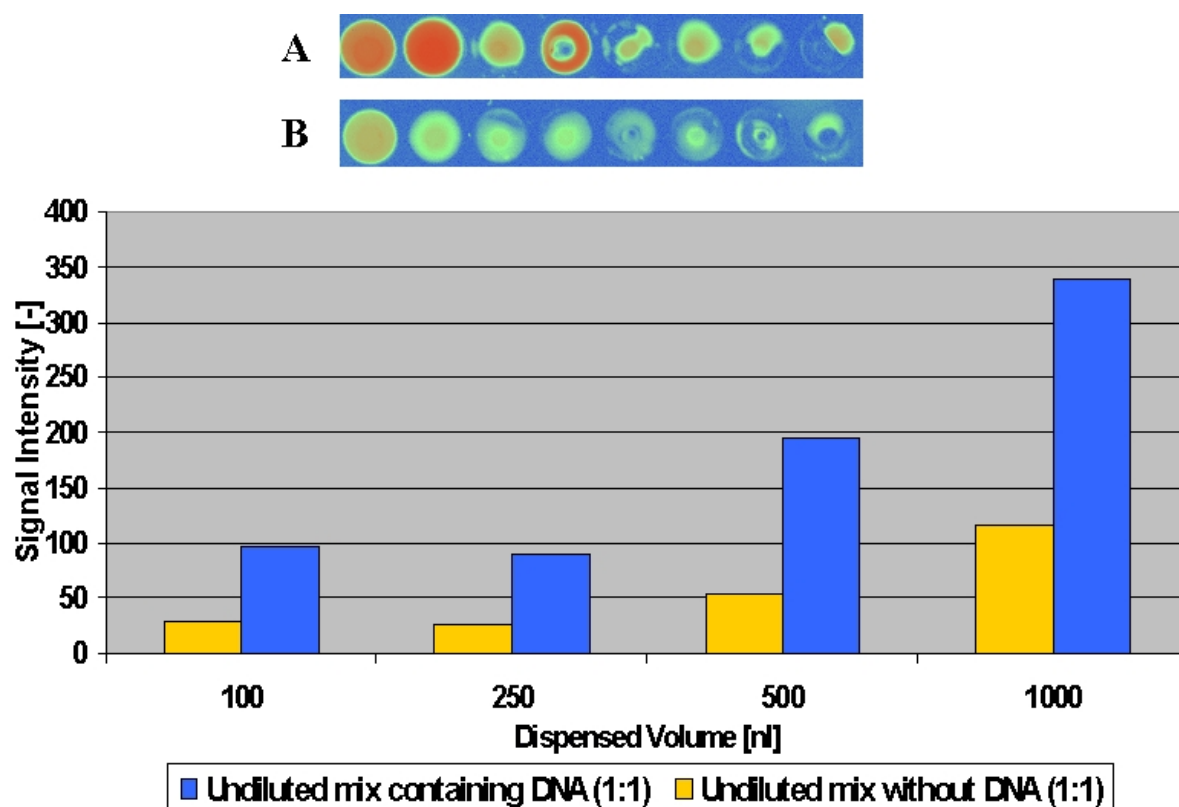


Figure 58: Scan of nanowells and diagram for the undiluted cell-free expression of GFP in the nanowell plate. Two batches were prepared, one with P_{T7} -GFP-DNA (A), one lacking DNA (B)

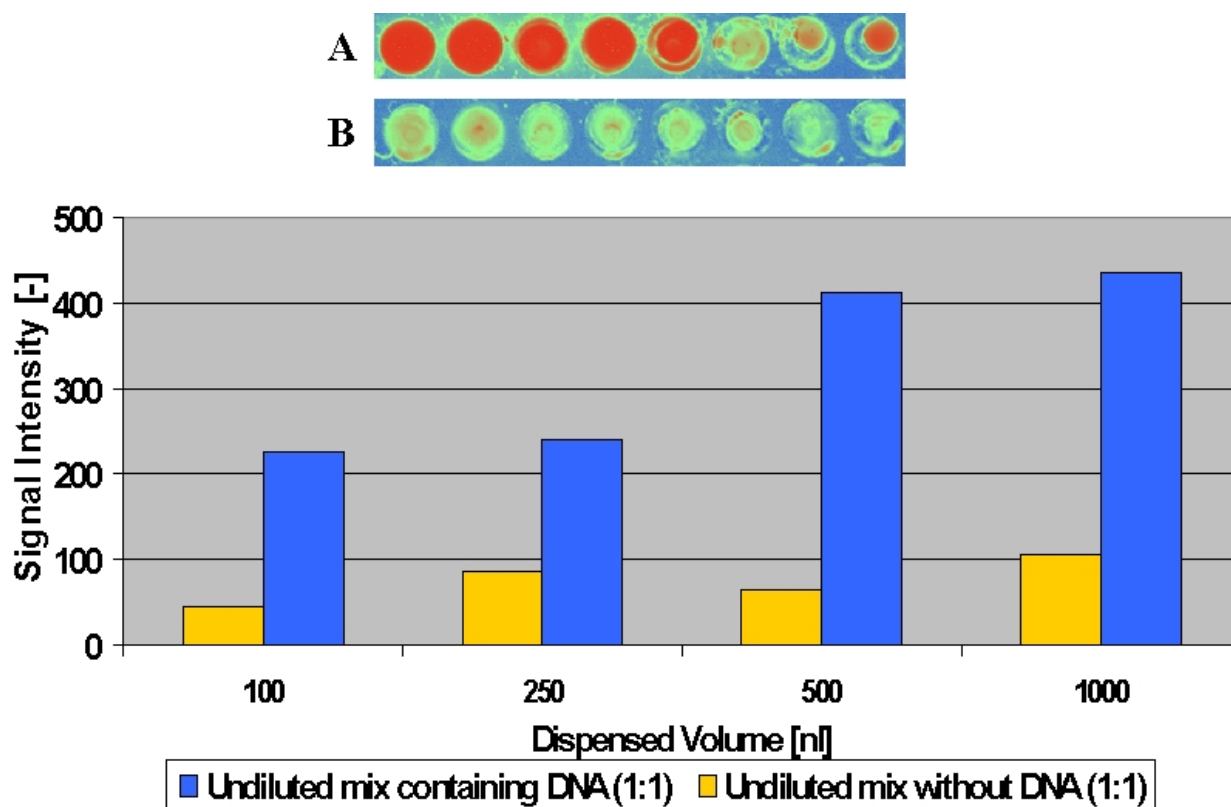


Figure 59: Scan of nanowells and diagram for the undiluted cell-free expression of β -galactosidase in the nanowell plate. Two batches were prepared, one with P_{T7} -GFP-DNA (A), one lacking DNA (B)

5.4.4 Enzyme Inhibition Assay in Nanowells

To show the usefulness of nanowell format and cell-free protein synthesis, an inhibition assay (Figure 60) with phenylethyl-D-thiogalactopyranoside (PETG) was performed, which is known to inhibit enzymatic activity of β -galactosidase (52, 134). The inhibition assay was performed in two approaches. In the first approach duplicates of 0.2 μ l of inhibitor with concentrations ranging from 333 μ M to 3.3 μ M was transferred into nanowells, followed by 0.6 μ l of a 1:10 diluted expression mix containing expressed β -galactosidase diluted in PBS and 0.2 μ l of 5 μ M FDG. As a positive control an additional reaction with PBS instead of inhibitor was performed. The second approach was performed exactly like the first approach with different inhibitor concentrations ranging from 33 μ M to 0.33 μ M.

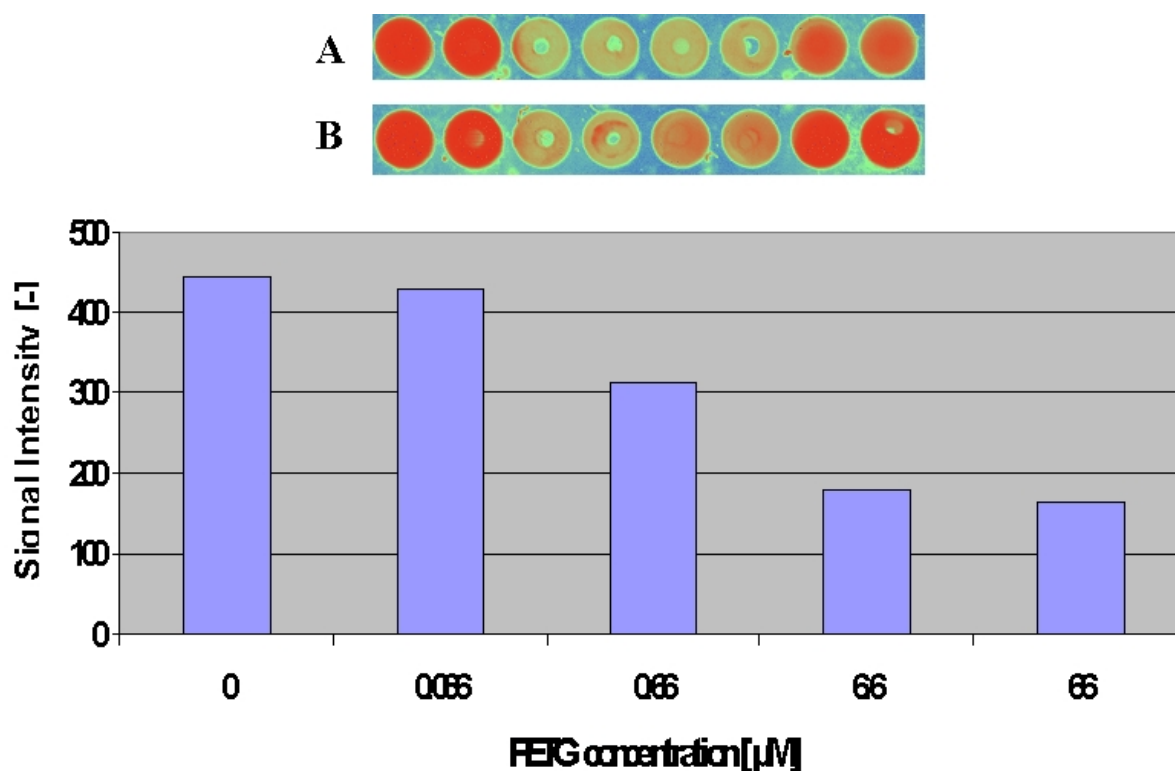


Figure 60: Scan of nanowells and diagram for the enzymatic inhibition assay in nanowells. (A) Assay with duplicates of PBS, 66 μ M, 6.6 μ M and 0.66 μ M PETG (from left to right). (B) Assay with duplicates of PBS, 6.6 μ M, 0.66 μ M and 0.066 μ M PETG